Molecular Therapy
Methods & Clinical Development
Original Article

# High-affinity chimeric antigen receptor signaling induces an inflammatory program in human regulatory T cells

Russell W. Cochrane,[1,2,3] Rob A. Robino,[1,2,3] Bryan Granger,[4] Eva Allen,[1,2,3] Silvia Vaena,[3] Martin J. Romeo,[3] Aguirre A. de Cubas,[1,3] Stefano Berto,[4,5] and Leonardo M.R. Ferreira[1,2,3]

[1]Department of Microbiology and Immunology, Medical University of South Carolina, Charleston, SC, USA; [2]Department of Regenerative Medicine and Cell Biology, Medical University of South Carolina, Charleston, SC, USA; [3]Hollings Cancer Center, Medical University of South Carolina, Charleston, SC, USA; [4]Bioinformatics Core, Medical University of South Carolina, Charleston, SC, USA; [5]Department of Neuroscience, Medical University of South Carolina, Charleston, SC, USA

**Regulatory T cells (Tregs) are promising cellular therapies to induce immune tolerance in organ transplantation and autoimmune disease. The success of chimeric antigen receptor (CAR) T cell therapy for cancer has sparked interest in using CARs to generate antigen-specific Tregs. Here, we compared CAR with endogenous T cell receptor (TCR)/CD28 activation in human Tregs. Strikingly, CAR Tregs displayed increased cytotoxicity and diminished suppression of antigen-presenting cells and effector T (Teff) cells compared with TCR/CD28-activated Tregs. RNA sequencing revealed that CAR Tregs activate Teff cell gene programs. Indeed, CAR Tregs secreted high levels of inflammatory cytokines, with a subset of FOXP3$^+$ CAR Tregs uniquely acquiring CD40L surface expression and producing IFN-γ. Interestingly, decreasing CAR antigen affinity reduced Teff cell gene expression and inflammatory cytokine production by CAR Tregs. Our findings showcase the impact of engineered receptor activation on Treg biology and support tailoring CAR constructs to Tregs for maximal therapeutic efficacy.**

## INTRODUCTION

Recent advancements in transplantation medicine and autoimmune disorder treatments have generated optimism for more effective and long-lasting therapies. Nevertheless, a significant drawback persists in the dependency on broad immunosuppressive therapies that are accompanied by various systemic side effects and significantly burden patients, including vulnerability to infections, cancer risk, hyperglycemia, multi-organ damage, and dependence on expensive lifelong treatments.[1–3] As a result, the demand for localized antigen-specific immunomodulatory strategies has never been more urgent.

Regulatory T cells (Tregs), a small (3%–6%) but indispensable subset of CD4$^+$ T cells, have emerged as a potential cornerstone for such targeted interventions.[4,5] Characterized by their unique cytokine and inhibitory receptor profiles and expression of the transcription factor FOXP3,[6–8] Tregs inhibit immune responses and promote tissue repair locally.[4,9] However, polyclonal Treg infusion in clinical settings for transplant and autoimmune disease has resulted in limited efficacy due to factors such as lack of antigen specificity, low abundance and expansion, functional instability upon *ex vivo* expansion, and limited *in vivo* survival.[5,10–12]

The groundbreaking success of chimeric antigen receptor (CAR) technology in oncology has propelled interest in its application to Tregs to solve the above-mentioned issues. CARs are designer proteins comprising an extracellular antigen-binding domain, typically an antibody-derived single-chain fragment variable (scFv), and an intracellular signaling domain, enabling T cell activation by an antigen of choice.[13] The success of CAR T cells in treating liquid tumors, with currently seven CAR T cell therapies approved by the US Food and Drug Administration,[14] has kindled interest in the generation of CAR Tregs to solve the problems of Treg antigen specificity and low numbers.

CAR Tregs have shown promise in preventing graft-vs.-host disease (GvHD) and skin graft rejection in humanized mouse models, as well as in preventing GvHD in immunocompetent mouse models.[15–19] Yet, CAR Tregs have displayed lackluster efficacy in solid organ transplant rejection and autoimmune disease in immunocompetent murine and non-human primate models, with CAR Tregs requiring combination with immunosuppressive molecules to show efficacy.[20,21] In addition, CAR Tregs have been either ineffective or only shown to prevent, not reverse, autoimmune disease in mouse models.[22–24] In contrast, allo-antigen-specific murine Tregs alone suffice to prevent acute and chronic rejection of skin allografts in C57BL/6 mice[25] and murine T cell receptor (TCR) transgenic islet antigen-specific BDC2.5 TCR Tregs not only prevent but also reverse autoimmune diabetes in non-obese diabetic mice.[26] Altogether, these preclinical data suggest that CAR Treg engineering and generation

Received 14 April 2024; accepted 14 November 2024;
https://doi.org/10.1016/j.omtm.2024.101385.

**Correspondence:** Leonardo M.R. Ferreira, Department of Microbiology and Immunology, Medical University of South Carolina, Charleston, SC, USA
**E-mail:** ferreirl@musc.edu

require further optimization for CAR Tregs to reach their full therapeutic potential. Moreover, reports that CAR Tregs can be cytotoxic toward target cells[19,27,28] have also cast doubt on their safety and invites discussion on target selection for CAR Treg-mediated immune protection. Recent clinical trials testing CAR Tregs in organ transplantation add urgency to a preemptive investigation into CAR Treg therapy safety and limitations.[29]

One plausible reason for the suboptimal performance of CAR Tregs lies in the fact that CAR constructs were originally designed and optimized for proinflammatory and cytotoxic T cells—a functional contradiction to the immunosuppressive nature of Tregs. TCR signaling is a complex cascade of events initiated by the engagement of the TCR with its cognate peptide-MHC complex on an antigen-presenting cell (APC), so called signal 1. Robust T cell activation requires an additional input, costimulation, or signal 2, which is typically transmitted upon the binding of CD28 on the T cell surface to CD80 or CD86 on the APC surface.[30] Notably, the TCR itself does not participate in signal transduction, relying instead on the associated CD3 protein complex containing CD3δ, CD3ε, and CD3γ, each with one immunoreceptor tyrosine-based activating motif (ITAM) signaling domain, and CD3ζ, which contains three ITAMs and thus transduces the strongest signal.[31] Strength and duration of this signaling ensemble orchestrate the functional outcomes of Treg activity, influencing their proliferation, immunosuppressive activity, and stability.[32–34] TCR signaling operates via a network of kinases, adaptor molecules, and transcription factors, ensuring a highly regulated and specific immune response. Current CAR constructs attempt to mimic this by containing signal 1 (CD3) and signal 2 (CD28) within the CAR intracellular signaling domain, leading to their simultaneous activation upon engagement of the CAR scFv with its target antigen.

Previous literature has predominantly focused on the binary outcomes of CAR Treg activation rather than delving into the nuanced functional outcomes of CAR Treg stimulation as compared with their TCR/CD28-stimulated counterparts. Such oversight could contribute to the observed suboptimal performance of CAR Tregs in preclinical settings, underlining the need for a comprehensive reevaluation. This study aims to bridge this gap, asking critical questions about the outcomes of CAR vs. endogenous TCR/CD28 signaling in Tregs. Specifically, what pathways might the current CAR constructs be missing or inappropriately triggering? By rigorously assessing these functional outcomes, we aim to optimize CAR Treg design, positioning it as a central element in the next generation of localized, antigen-specific immunomodulatory strategies.

Utilizing a variety of assays and techniques, we compare the activation, function, stability, and gene expression profiles of engineered CAR Tregs with those of endogenously activated TCR/CD28 Tregs. Our investigation uncovered substantial alterations in Treg phenotype and function upon CAR-mediated activation, notably a shift toward a more inflammatory and cytotoxic gene expression profile and behavior. Indeed, we found *de novo* expression of CD40L as a surface marker associated with a subset of proinflammatory CAR Tregs. Finally, we identified scFv affinity as a CAR design parameter that modulates CAR Treg inflammatory cytokine production, with Treg activation via a lower-affinity CAR resulting in a cytokine expression profile closer to that of TCR/CD28-activated Tregs.

## RESULTS

### Human CAR Treg generation

To systematically evaluate the phenotypic and functional discrepancies between CAR and endogenous TCR/CD28-mediated activation of human Tregs, we used a well-established anti-human CD19 CAR construct[35] with minor modifications, featuring an N terminus Myc-tag to assess CAR surface expression, a CD28-CD3ζ signaling domain, and a green fluorescent protein (GFP) reporter gene to identify CAR-expressing cells (Figure S1A). We then magnetically isolated $CD4^+$ T cells and $CD8^+$ T cells from human peripheral blood (Figure S1B) and used fluorescence-assisted cell sorting (FACS) to further purify $CD4^+CD25^{hi}CD127^{low}$ Tregs[36,37] and $CD4^+CD25^{low}CD127^{hi}$ effector T (Teff) cells from the $CD4^+$ T cells (Figure S1C). Isolated cells were activated with anti-CD3/CD28 beads and interleukin-2 (IL-2), transduced with CAR lentivirus 2 days later, and expanded in the presence of IL-2. As expected, Tregs co-expressed the Treg lineage transcription factors FOXP3 and HELIOS,[11,15] whereas Teff cells did not (Figure S1C). CAR-expressing cells were isolated by FACS based on GFP expression and CAR surface expression on the isolated cells confirmed using flow cytometry (Figure S1D). Expanded CAR Tregs were then used for experiments 9–13 days after initial anti-CD3/CD28 bead activation (Figure S1B).

### CAR Tregs are functionally distinct from endogenous TCR/CD28-activated Tregs

To compare endogenous TCR/CD3 complex and CD28 stimulation with CAR stimulation, we generated target cell lines to elicit either TCR/CD28 or CAR activation. Specifically, we transduced either a CD64-2A-CD80 or a CD19 extracellular domain fused to a platelet-derived growth factor (PDGFR) transmembrane transgene into K562 cells, a human myelogenous leukemia cell line that lacks human leukocyte antigen (HLA), CD80, and CD86 expression and thus does not activate T cells. CD64 is a high-affinity Fc receptor and CD80 binds to CD28. CD64-expressing K562 cells were loaded with anti-CD3 antibody, as described previously,[38] to activate Tregs via the TCR. Expanded CAR Tregs were incubated with irradiated K562 cells (no activation, "No Act"), irradiated CD64-CD80-K562 cells decorated with anti-CD3 antibody (TCR/CD28 activation), or irradiated CD19-K562 cells (CAR activation) (Figures 1A, S2A, S2B, and S2D). With this setup, we could compare endogenous CD3 (bound by anti-CD3) and endogenous CD28 (bound by CD80) stimulation with CD3 and CD28 stimulation delivered by CAR (containing a CD28-CD3ζ signaling domain and bound by CD19) in human Tregs, with both modes of stimulation being delivered by a target cell, not an artificial bead.

Our first aim was to investigate whether stimulation via a CD28-CD3ζ CAR or endogenous TCR/CD3 and CD28 pathways results

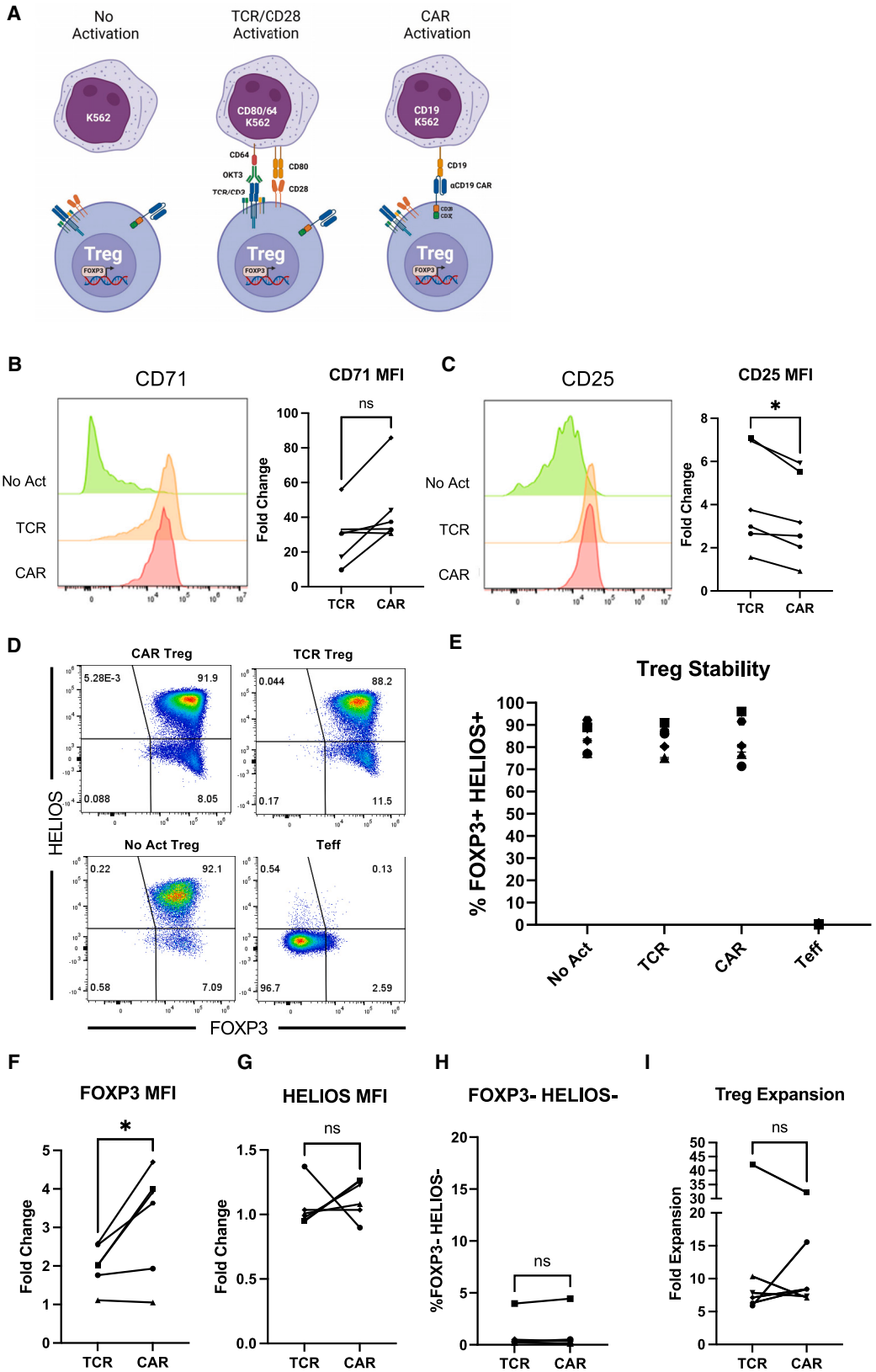


*(legend on next page)*

in different levels of Treg activation. To assess this, CAR Tregs were coincubated with each K562 cell line, harvested after 48 h, and their activation status was evaluated by measuring the cell surface expression of CD71 (transferrin receptor), a well-established marker of T cell activation. Interestingly, no statistically significant difference was found in the mean fluorescence intensity of CD71 between CAR- and TCR/CD28-activated Tregs across blood donors (Figure 1B).

In parallel, we examined the expression of CD25, the high-affinity α chain of the IL-2 receptor. In addition to being a T cell activation marker, CD25 is constitutively expressed by Tregs and is crucial for their immunosuppressive function via IL-2 sequestration.[4,39] We were intrigued to find that TCR/CD28-activated Tregs had slightly but significantly higher levels of CD25 expression compared with CAR-activated Tregs after 48 h of coculture (Figure 1C).

Next, we assessed the stability of the Treg phenotype on day 8 post-activation, as Tregs can convert into effector-like cells under certain conditions, such as highly inflammatory microenvironments and repeated *in vitro* stimulation.[40–42] To gauge this, we assessed the expression of the Treg lineage transcription factors FOXP3 and HELIOS. FOXP3 is indispensable for Treg identity and function,[6–8] while HELIOS is believed to confer stability to the Treg phenotype.[43] Across blood donors, we found that all activation conditions maintained a distinct (Figure 1D) and equally abundant (Figure 1E) $FOXP3^{+}HELIOS^{+}$ cell population, indicating that neither CAR nor TCR/CD28 activation led to Treg destabilization. Indeed, FOXP3 levels were higher in CAR- vs. TCR/CD28-activated Tregs (Figure 1F), HELIOS levels were similar (Figure 1G), and the frequency of $FOXP3^{-}HELIOS^{-}$ Teff cell population was equally low in CAR- and TCR/CD28-activated Tregs (Figure 1H).

To complete this initial phenotypic characterization, we evaluated the cells' expansion capacity–a critical attribute considering the current challenges in achieving therapeutically sufficient Treg numbers for infusion.[11] In line with activation and stability, expansion of CAR- and TCR/CD28-activated Tregs was similar across donors (Figure 1I).

While phenotypic characterization indicated that CAR-activated Tregs closely resemble TCR/CD28-activated Tregs, functional assays are essential to characterize these modes of activation. Tregs have an arsenal of over a dozen known suppressive mechanisms, inhibiting immune responses both through contact-independent pathways–such as the sequestration of IL-2 via CD25 and the secretion of anti-inflammatory cytokines such as IL-10 and contact-dependent pathways, such as CTLA4-mediated trogocytosis of costimulatory molecules CD80 and CD86 from APCs.[4,44]

To delineate how CAR activation influences these functionalities compared with endogenous TCR/CD28 activation, we first employed a modified *in vitro* T cell suppression assay where Tregs were activated via CAR or TCR/CD28 overnight and then co-incubated with CellTrace dye-labeled $CD4^{+}$ and $CD8^{+}$ T responder (Tresp) cells activated with anti-CD3/CD28 beads overnight in parallel at different Treg to Tresp cell ratios.[45,46] Interestingly, CAR-activated Tregs were less efficacious than their TCR/CD28-activated counterparts in inhibiting $CD4^{+}$ (Figure 2A) and $CD8^{+}$ (Figure 2B) Tresp cell proliferation. In addition, to assess APC modulatory activity, we co-incubated CAR Tregs with CD64-CD80-NALM6 (Figure S2C), with NALM6 being a $CD19^{+}$ B cell leukemia cell line, to provide CAR activation by a target cell expressing CD80. In parallel, untransduced (UT) Tregs were co-incubated with the same CD64-CD80-NALM6 target cell line but loaded with anti-CD3 antibody to provide endogenous TCR/CD28 activation. Four days later, CD80 surface expression was measured by flow cytometry.[47] Consistent with our observations on T cell suppression (Figures 2A and 2B), CD80 expression on the target cells was downregulated to a lesser extent by CAR Tregs than by their TCR/CD28-activated counterparts (Figures 2C and 2D).

Despite not being as studied as other Treg-suppressive strategies, Tregs have been found to suppress immune responses via direct cytotoxicity. The most common mechanism of cytotoxicity by T cells and natural killer (NK) cells is the perforin/granzyme pathway, where perforin forms pores in the membrane of the target cells, allowing the delivery of granzymes into the target cells and subsequent induced cell death.[48] Tregs have been shown to kill their target cells via the perforin/granzyme pathway. Indeed, both granzymes and perforin are required for optimal Treg-mediated suppression *in vivo*, as Tregs utilize these molecules to directly eliminate B cells, dendritic cells (DCs), $CD8^{+}$ T cells, and NK cells.[49–52] Considering that CAR signaling was initially designed for triggering inflammatory responses and cytotoxicity by Teff cells, we hypothesized that CAR Tregs might be more cytotoxic than TCR/CD28-activated Tregs. To test this, we again incubated CAR Tregs with NALM6 and untransduced Tregs with

**Figure 1. CAR and endogenous TCR/CD28 activation result in phenotypically similar Tregs**

(A) Three modes of activation used in this study: No Activation with target K562 cells (No Act), TCR/CD28 activation with target K562 cells expressing CD64 loaded with anti-CD3 antibody and CD80 (TCR), and CAR activation with target K562 cells expressing CD19 (CAR). (B) CD71 surface expression 48 h after Treg activation. Representative histograms on the left and summary data across donors of fold change in CD71 mean fluorescence intensity (MFI) in relation to No Act Tregs on the right. (C) CD25 surface expression 48 h after Treg activation. Representative histograms on the left and summary data across donors of fold change in CD25 MFI in relation to No Act Tregs on the right. (D) Representative dot plots of FOXP3 and HELIOS expression in CAR Treg, TCR Treg, and No Act Treg, as well as in Teff cells as a negative staining control 8 days post-activation. (E) Percentage of $FOXP3^{+}HELIOS^{+}$ cells across activation modes and donors 8 days post-activation. (F) Fold change in FOXP3 MFI in TCR Tregs or CAR Tregs over No Act Tregs across donors. (G) Fold change in HELIOS MFI in TCR Tregs or CAR Tregs over No Act Tregs across donors. (H) Percentage of $FOXP3^{-}HELIOS^{-}$ cells across activation modes and donors 8 days post-activation. (I) Fold expansion in cell number for TCR Tregs and CAR Tregs 1 week post-activation. For (B and C) and (F–I), values represent mean of technical triplicates per blood donor ($n = 6$), with lines collecting the data points from the same donor. For (E), values represent mean ± standard deviation (SD) of technical triplicates per blood donor ($n = 6$). Paired Student's t test. *$p < 0.05$; ns, not significant.

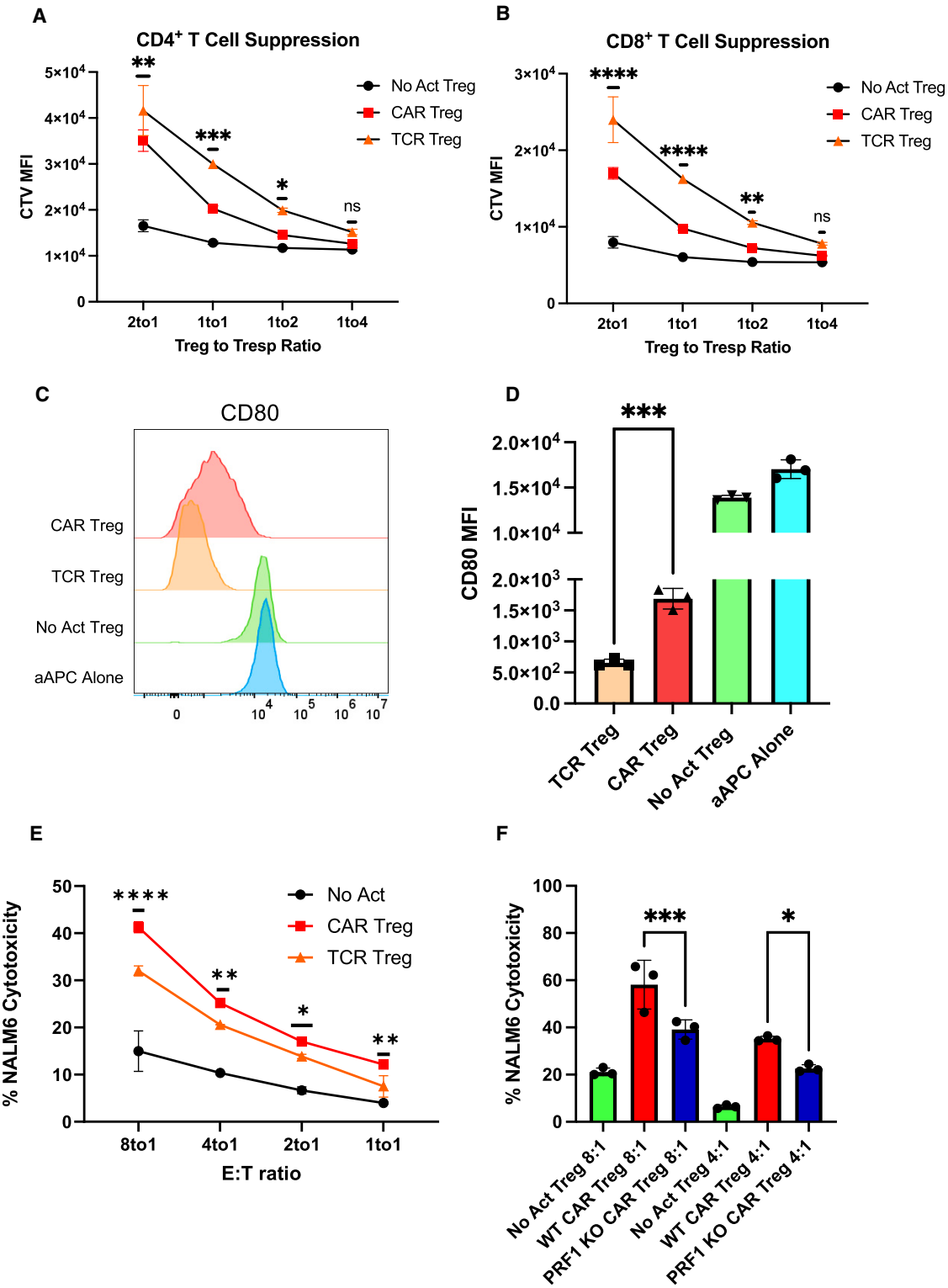


**Figure 2. CAR activation leads to a shift from suppression to cytotoxicity in Tregs**

(A) Inhibition of CellTrace Violet (CTV)-labeled CD4$^+$ T responder cell (Tresp) proliferation by Tregs. (B) Inhibition of CTV-labeled CD8$^+$ Tresp proliferation by Tregs. (C) Representative histograms of downregulation of CD80 surface expression in CD80-CD64-NALM6 cells (aAPC, artificial antigen-presenting cells) by Tregs. (D) Summary data

*(legend continued on next page)*

CD80-CD64-NALM6 loaded with anti-CD3 antibody to test CAR activation and TCR/CD28 activation, respectively. In agreement with our hypothesis, CAR Tregs were significantly more cytotoxic than TCR/CD28-activated Tregs toward NALM6 cells at different effector to target (E:T) ratios (Figure 2E). In contrast, CAR Teff and TCR/CD28-activated Teff cells were equally as cytotoxic toward NALM6 cells. (Figure S2E). To investigate whether CAR Treg cytotoxicity was exacerbated through the perforin/granzyme pathway, we deleted the *PRF1* gene, which encodes perforin, in CAR Tregs using CRISPR-Cas9 and evaluated the cytotoxicity of the CAR Tregs toward NALM6 cells. Indeed, *PRF1* knockout CAR Tregs (59% indel efficiency by tracking of indels by decomposition [TIDE] analysis[53]) were less effective at killing NALM6 cells than their wild-type (WT) counterparts (Figure 2F). In addition, we investigated whether CAR Tregs could eliminate non-immune cells. Most CAR Treg therapies currently being investigated directly target the tissues to be protected from immune rejection.[29] Hence, it is fundamental to ask whether CAR Tregs protect the targeted tissue rather than participating in its elimination. To answer this question, we ectopically expressed our CD19 extracellular domain fused to a PDGFR transmembrane transgene in A549 lung cancer epithelial cells. Interestingly, CAR Tregs were not cytotoxic toward CD19-A549 cells, in contrast with CAR Teff cells (Figure S2F), suggesting that CAR Tregs may not eliminate non-immune cells expressing the CAR target.

### CAR activation induces a unique transcriptome in Tregs

Given our observations on CAR-activated Tregs' enhanced cytotoxicity and reduced suppressive function in comparison with endogenous TCR/CD28-activated Tregs, a crucial question emerged: Why do these alterations occur? Answering this question holds significance not only for our understanding of Treg biology but also for the efficacy of CAR Tregs in the clinic. To address this question, we co-incubated CAR Tregs or CAR Teff cells with each of the three types of irradiated target K562 cell lines; No Act, TCR/CD28 activation ("TCR"), and CAR activation ("CAR") and then performed RNA sequencing (RNA-seq) on $CD4^+$ T cells isolated 24 h post-activation. Whole-transcriptome analysis with two blood donors under all six conditions revealed that both CAR- and TCR/CD28-activated Tregs upregulated *NR4A1* and *NR4A3*, which are immediate-early genes induced by TCR signaling[54]; *IL10* and *EBI3*, which encode the anti-inflammatory cytokines IL-10 and IL-35,[55,56] respectively; *CCR8*, a chemokine receptor gene expressed in highly activated Tregs[57]; and *IL1R2*, a gene that encodes a decoy receptor for the inflammatory cytokine IL-1[58] (Tables S1 and S2). However, relative to No Act Tregs, 3,680 genes were upregulated by CAR activation in Tregs (Table S1), while only 1,236 genes were upregulated in response to TCR/CD28 activation (Table S2), suggesting that CAR activation elicits a more pronounced transcriptional response in Tregs than does endogenous TCR/CD28 signaling. Of note, a similar pattern was observed in Teff cells, with CAR activation upregulating 4,013 genes compared with 2,058 genes with TCR/CD28 activation (Tables S3 and S4). Interestingly, CAR Treg and CAR Teff cells clustered closest together despite being different cell types (Figure 3A). In line with this observation, joint analysis of genes upregulated by CAR Tregs, TCR Tregs, CAR Teff, and TCR Teff in comparison with the respective non-activated cells revealed that CAR Tregs shared 1,038 uniquely upregulated genes with CAR Teff but only 219 uniquely upregulated genes with TCR Tregs (Figure 3B). These findings suggested that CAR activation induces the expression of Teff cell gene programs in Tregs, as if CAR signaling partly overrides intrinsic Treg gene programs. Indeed, the top differentially expressed protein-coding genes between CAR Tregs and TCR Tregs (Table S5) included key proinflammatory cytokine and chemokine genes, such as *IFNG*, *IL17F*, *IL3*, *CCL3*, *CCL19*, and *CSF3* (Figure 3C). Gene set enrichment analysis (GSEA)[59] revealed that the upregulated gene programs in CAR Tregs in comparison with those in TCR Tregs were primarily those related to cytokine signaling and inflammation, such as PI3K-AKT signaling, IL-17 signaling, cytokines and inflammatory response, and proinflammatory and profibrotic mediators, as well as those involved in hematopoietic cell lineage differentiation (Figure 3D), with CAR Tregs expressing higher levels of proinflammatory cytokine and chemokine genes than TCR Tregs. Curiously, CAR activation also resulted in differences in chemokine receptor gene expression: while the expression of *CCR2* and *CCR5*, high in TCR Tregs, was even lower in CAR Tregs than in CAR Teff and TCR Teff cells (Figure S3A), *CCR8* expression, absent in Teff cells, was even higher in CAR Tregs than in TCR Tregs (Figure S3A).

### CAR activation induces a distinct cytokine production pattern in Tregs

Considering the marked increased in proinflammatory cytokine and chemokine gene expression by CAR Tregs compared with TCR/CD28-activated Tregs, we sought to validate this pattern at the protein level. First, we collected the supernatants of 48 h co-cultures of CAR Tregs and CAR Teff cells with either irradiated K562 cells (no activation), irradiated CD64-CD80-K562 cells with anti-CD3 (TCR/CD28 activation), or irradiated CD19-K562 cells (CAR activation) for cytokine quantitation using multiplex enzyme-linked immunosorbent assay (ELISA). CAR Tregs secreted more shed CD40L (sCD40L), IFN-γ, IL-17A, and IL-13 than TCR/CD28 Tregs while secreting similar amounts of TNF-α and IL-10 (Figure 4A). CAR Tregs also secreted more IL-3, G-CSF, IL-4, IL-6, and TNF-β than TCR Tregs (Figure S3B). Overall, these cytokine secretion data echoed our RNA-seq data, suggesting that CAR activation leads to notably higher inflammatory cytokine and chemokine production in Tregs while maintaining immunosuppressive cytokine secretion levels. One of the most intriguing findings from the cytokine quantification was IFN-γ secretion by CAR Tregs, reaching levels

of downregulation of CD80 surface expression in CD80-CD64-NALM6 cells. (E) Treg cytotoxicity toward target NALM6 cells at different effector to target (E:T) ratios. (F) WT and *PRF1* KO CAR Treg cytotoxicity toward target NALM6 cells at different E:T ratios. Values represent technical replicates of representative experiments. Bars represent mean ± SD. Statistical significance was determined using two-way ANOVA (A, B, and E), unpaired Student's t test (D), or one-way ANOVA (F) with Tukey's multiple comparison correction. $^{****}p < 0.0001$, $^{***}p < 0.001$, $^{**}p < 0.01$, $^{*}p < 0.05$; ns, not significant.

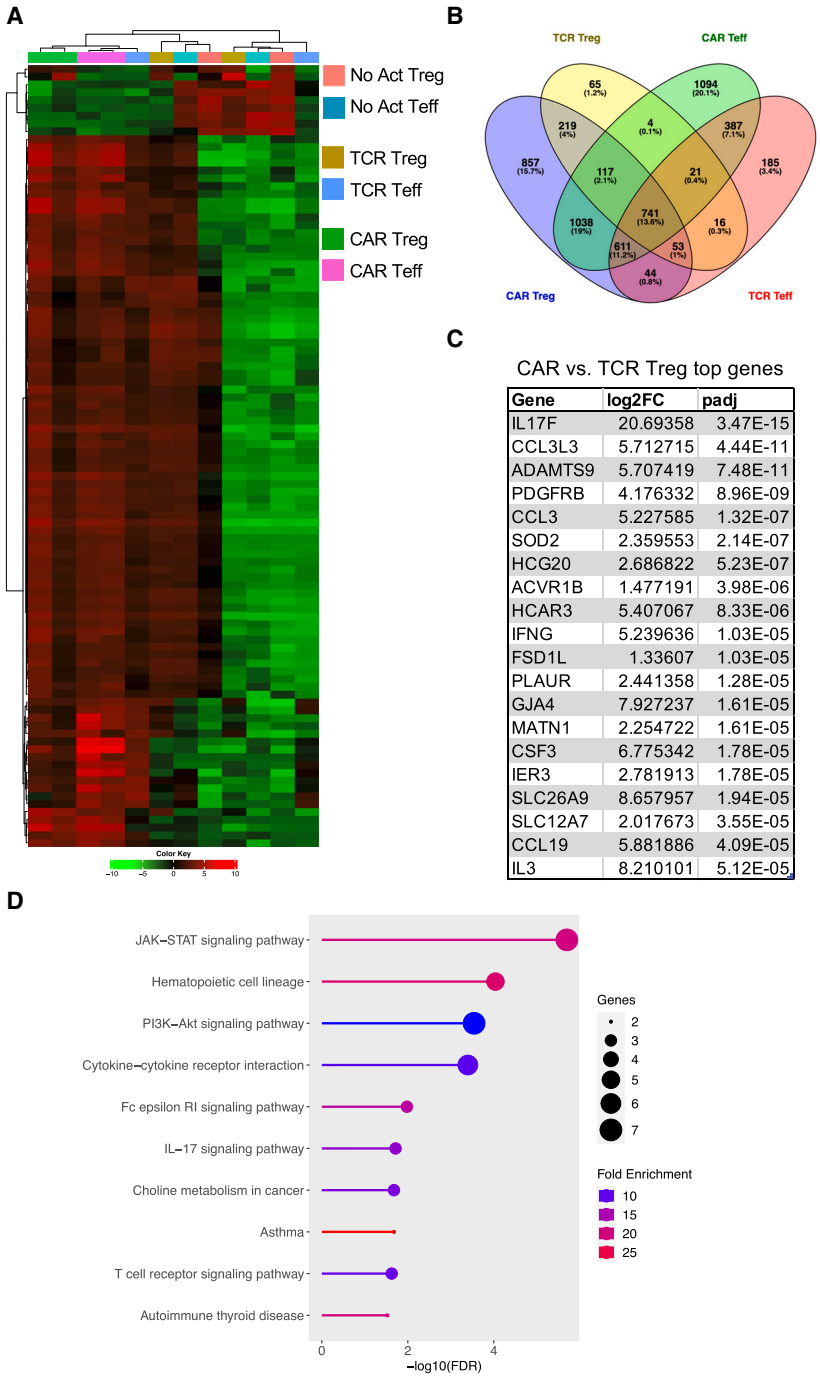


| Gene | log2FC | padj |
|---|---|---|
| IL17F | 20.69358 | 3.47E-15 |
| CCL3L3 | 5.712715 | 4.44E-11 |
| ADAMTS9 | 5.707419 | 7.48E-11 |
| PDGFRB | 4.176332 | 8.96E-09 |
| CCL3 | 5.227585 | 1.32E-07 |
| SOD2 | 2.359553 | 2.14E-07 |
| HCG20 | 2.686822 | 5.23E-07 |
| ACVR1B | 1.477191 | 3.98E-06 |
| HCAR3 | 5.407067 | 8.33E-06 |
| IFNG | 5.239636 | 1.03E-05 |
| FSD1L | 1.33607 | 1.03E-05 |
| PLAUR | 2.441358 | 1.28E-05 |
| GJA4 | 7.927237 | 1.61E-05 |
| MATN1 | 2.254722 | 1.61E-05 |
| CSF3 | 6.775342 | 1.78E-05 |
| IER3 | 2.781913 | 1.78E-05 |
| SLC26A9 | 8.657957 | 1.94E-05 |
| SLC12A7 | 2.017673 | 3.55E-05 |
| CCL19 | 5.881886 | 4.09E-05 |
| IL3 | 8.210101 | 5.12E-05 |

**Figure 3. CAR activation induces proinflammatory gene programs in Tregs**

(A) Heatmap clustered by column (sample) and by row (gene) with top 100 most differentially expressed genes between No Act Tregs, TCR Tregs, CAR Tregs, No Act Teff, TCR Teff, and CAR Teff. (B) Venn diagram with genes upregulated in TCR Tregs, CAR Tregs, TCR Teff, and CAR Teff in relation to their respective No Act cell types. Number of genes and respective percentage of the total number of genes are indicated in each intersection. (C) Top 20 protein-coding genes most differentially expressed in CAR Tregs compared with TCR Tregs. FC, fold change; padj, adjusted *p* value. (D) KEGG pathway gene set enrichment analysis (GSEA) of CAR Tregs vs. TCR Tregs. FDR, false discovery rate.

comparable with those of CAR Teff and TCR Teff cells (Figure 4A), in line with *IFNG* being one of the most differentially expressed genes between CAR Tregs and TCR Tregs (Figure 3C). Even though our Treg lineage stability analysis indicated that CAR-activated Tregs retained FOXP3 and HELIOS expression to the same extent as TCR/CD28-activated Tregs (Figures 1D–1H), we set out to examine whether the high IFN-γ levels measured using bulk RNA-seq and ELISA were the product of contaminating Teff cells and/or FOXP3 negative ex-Treg cells. We performed intracellular cytokine staining for CAR Tregs and CAR Teff cells following no activation, CAR activation, or TCR/CD28 activation with the respective target K562 cell lines overnight followed by 5 h of brefeldin A and found that CAR-activated FOXP3$^+$ Tregs, but not TCR/CD28-activated Tregs, produced IFN-γ (Figure 4B), suggesting that CAR Tregs do not become unstable and lose Treg identity before producing IFN-γ. In line with this hypothesis, Tregs did not produce IL-2 regardless of activation mode (Figure 4C), a key hallmark of Treg identity.[60] In contrast, Teff cells produced IFN-γ (Figure 4B) and IL-2 (Figure 4C) when activated via CAR or endogenous TCR/CD28, as expected. Therefore, CAR activation generates a unique subset of Tregs that are proinflammatory yet retain key Treg identity markers. This implies that CAR activation is leading to the emergence of a functionally distinct Treg subpopulation that can potentially influence the balance of immune responses in novel ways.

## Characterizing the proinflammatory CAR Treg subset

As we delved deeper into understanding CAR Tregs' unique functional attributes, we recognized the importance of investigating cell surface markers. In addition to being important phenotypic signposts, surface markers can be used to better identify and purify cell subsets, allowing for a more nuanced understanding of CAR Tregs. Upon scrutinizing our RNA-seq data, specifically the genes upregulated in different modes of activation (CAR vs. TCR/CD28) and cell types (Treg vs. Teff) (Figure 3B), we noticed that CAR Tregs, CAR Teff, and TCR Teff, but not TCR Tregs, upregulated *CD40LG* (Table S6), a gene coding for the well-known Teff cell activation markers CD40L or CD154.[61]

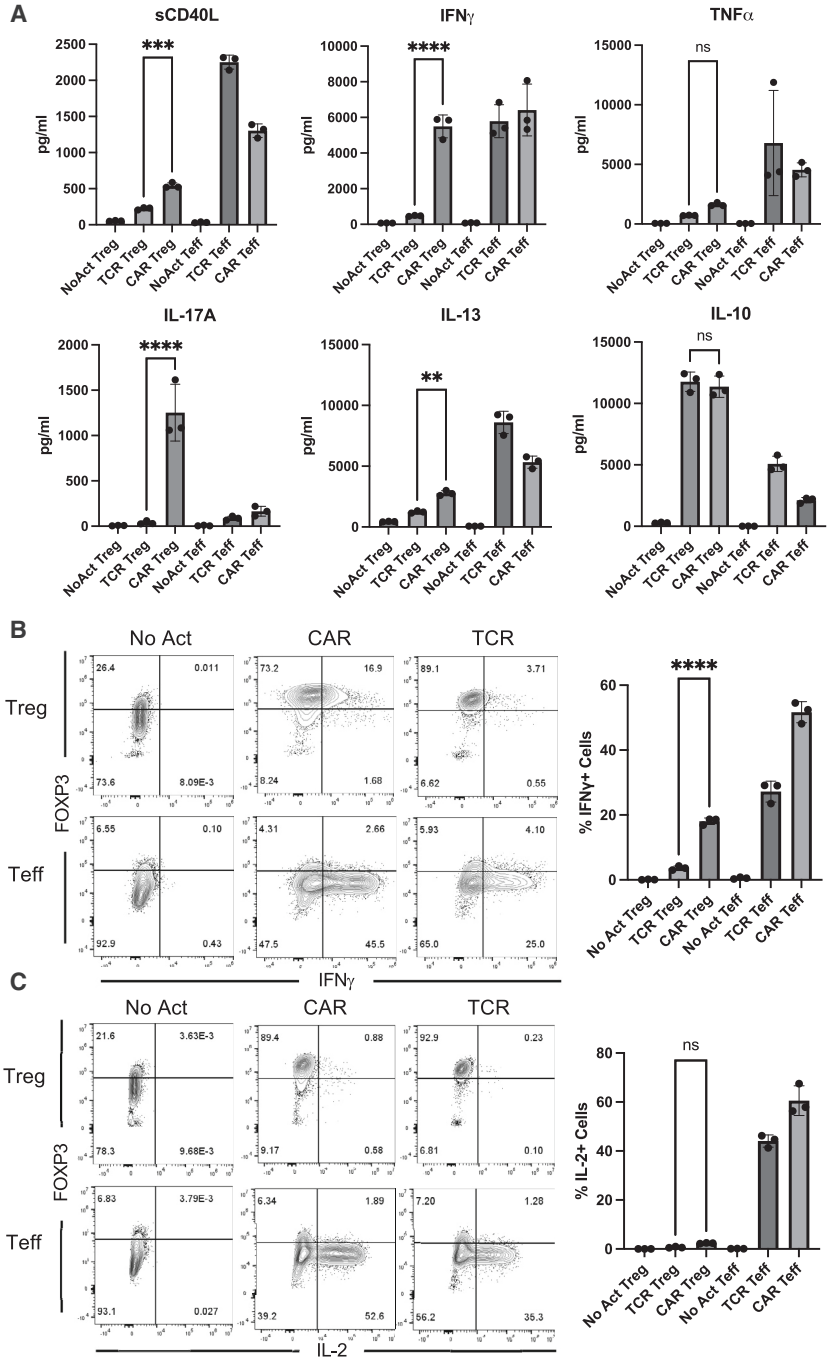


**Figure 4. CAR Tregs uniquely produce inflammatory cytokines**

(A) Levels of cytokines secreted by No Act Tregs, TCR Tregs, CAR Tregs, No Act Teff, TCR Teff, and CAR Teff 48 h post-activation. (B) Intracellular levels of IFN-γ produced by No Act Tregs, TCR Tregs, CAR Tregs, No Act Teff, TCR Teff, and CAR Teff 18 h post-activation. Representative contour plots on the left and summary data on the right. (C) Intracellular levels of IL-2 produced by No Act Tregs, TCR Tregs, CAR Tregs, No Act Teff, TCR Teff, and CAR Teff 18 h post-activation. Representative contour plots on the left and summary data on the right. Values represent technical replicates of representative experiment. Bars represent mean ± SD. One-way ANOVA with Tukey's multiple comparison correction. $^{****}p < 0.0001$, $^{***}p < 0.001$, $^{**}p < 0.01$, $^{*}p < 0.05$; ns, not significant.

In addition, CAR Tregs secreted significantly more sCD40L than TCR/CD28-activated Tregs (Figure 4A). Conversely, TCR Tregs, but not any of the other three activated conditions, upregulated *FCRL3* and *ENTPD1* (Table S7). *ENTPD1* encodes CD39, a cell surface ectoenzyme expressed in Tregs that converts ATP into the immunosuppressive molecule adenosine.[62] Yet, TCR Tregs also uniquely upregulated *ENTPD1-AS1* (Table S7), an anti-sense RNA previously shown to decrease CD39 expression.[63] FCRL3, on the other hand, has been associated with TIGIT and HELIOS expression in Tregs.[64] TIGIT is a surface marker expressed by Tregs that are highly suppressive toward Th1 cells, which secrete IFN-γ, and Th17 cells, which secrete IL-17.[65] Molecularly, TIGIT is thought to induce phosphatase activity to downmodulate TCR signaling in the TIGIT-expressing Treg and to induce IL-10 production by DCs upon binding to PVR on the surface of the DC.[66] Although not statistically significant ($p > 0.05$), TCR/CD28-activated Tregs upregulated *TIGIT* transcript (Table S1), whereas CAR-activated Tregs did not (Table S2).

We then aimed to validate whether CD40L and TIGIT were differentially expressed in CAR- and TCR/CD28-activated Tregs at the surface protein level using flow cytometry, possibly offering a further detailed characterization of the unique proinflammatory CAR Treg phenotype. Following a 48-h activation, CAR Tregs displayed significantly higher CD40L and reduced TIGIT levels compared with TCR Tregs (Figure 5A), trends that were maintained 1 week after activation (Figure 5B). A targeted gene expression survey using quantitative polymerase chain reaction (qPCR) following 24 h activation confirmed that CAR Tregs express higher levels of the Teff cell genes *IFNG*, *GZMB*, and *CD40LG*, and lower levels of *TIGIT* than TCR/CD28-activated Tregs (Figure 5C). Yet, CAR Tregs did not express higher levels of *TBX21*, *GATA3*, or *RORC*, genes coding for the master transcription factors T-BET, GATA3, and RORγT of the main $CD4^+$ Teff cell lineages Th1, Th2, and Th17, respectively, or *STAT1*, a gene coding for a key transcription factor in IFN-γ signaling[67,68] (Figure 5C).

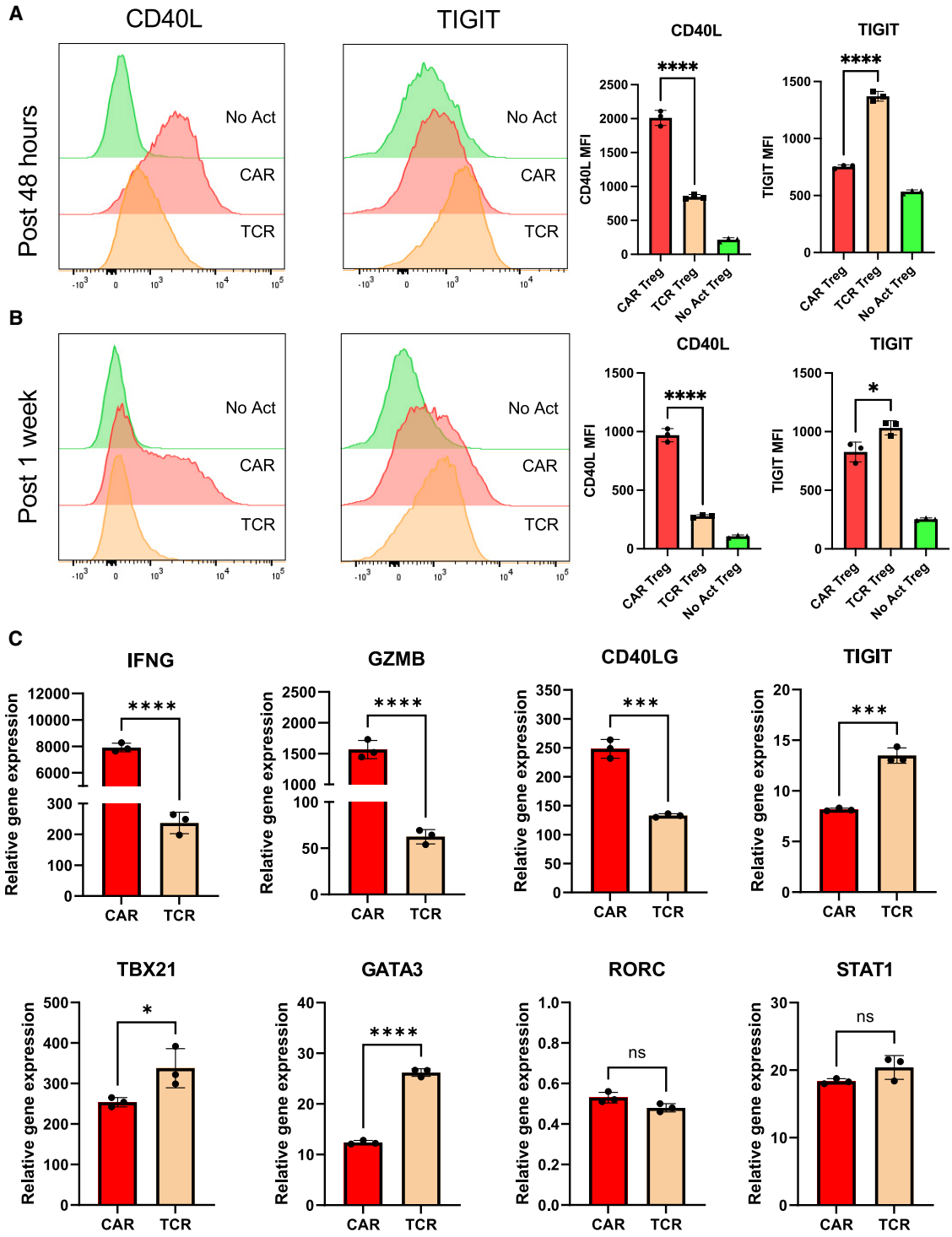


**Figure 5. CAR activation induces CD40L expression in Tregs**

(A) CD40L and TIGIT surface expression on No Act Tregs, TCR Tregs, and CAR Tregs 48 h post-activation. Representative histograms on the left and summary data on the right. (B) CD40L and TIGIT surface expression on No Act Tregs, TCR Tregs, and CAR Tregs 1 week post-activation. Representative histograms on the left and summary data on the right. (C) Expression of selected genes in CAR Tregs and TCR Tregs 24 h post-activation, evaluated by qPCR. Bars represent mean ± standard deviation (SD) technical replicates of representative experiment. Statistical significance was determined using one-way ANOVA with Tukey's multiple comparison correction (A and B) and unpaired Student's t test (C). ****$p < 0.0001$, ***$p < 0.001$, **$p < 0.01$, *$p < 0.05$; ns, not significant.

### Naive and memory Tregs are equally susceptible to secreting inflammatory cytokines upon CAR activation

Strategies to obtain human Treg subpopulations that maximize immunosuppressive properties and minimize destabilization have been an ongoing effort in the field to reach therapeutic efficacy. However, sorting subpopulations from an already scarce population may aggravate the ongoing difficulties in reaching a clinical minimal infusible dose in Treg therapy trials.[11] Still, understanding the proliferative, stability, and immunosuppressive properties of different Treg subsets can provide insights into how to engineer Tregs effectively. Recent studies in the CAR Treg field have utilized naive ($CD45RA^+$ $CD45RO^-$) Tregs, given their potential to be less prone to destabilization, i.e., loss of FOXP3 expression, than memory ($CD45RA^+$ $CD45RO^-$) Tregs, aiming at a cell product with lower Teff cell contamination for infusion.[69–72] Moreover, while memory Tregs tend to be more frequent in adults,[73] naive Tregs have greater proliferative potential after the first round of stimulation *ex vivo*.[69,72] Given our revelation that CAR stimulation induces a heightened production of cytolytic mediators and effector cytokines and the fact that memory Tregs have been reported to produce significantly greater amounts of effector cytokines than naive Tregs,[69,70] we aimed to test whether utilizing only the naive fraction of peripheral blood Tregs rather than bulk Tregs would minimize inflammatory cytokine secretion induced by CAR stimulation in human Tregs. As expected, both FACS sorted $CD4^+CD25^{hi}CD127^{low}CD45RA^+CD45RO^-$ naive Tregs and $CD4^+CD25^{hi}CD127^{low}CD45RA^-CD45RO^+$ memory Tregs co-expressed the Treg lineage transcription factors FOXP3 and HELIOS (Figure S4A). Upon co-incubation with irradiated CD19-562 cells for 48 h, there was no difference between CAR naive Tregs and CAR memory Tregs in activation status, as assessed by CD71 upregulation (Figures S4B and S4D), or CD40L surface expression (Figures S4C and S4E). In addition, there was no difference in the frequency of $FOXP3^+HELIOS^+$ cells or the expression level of FOXP3 and HELIOS between CAR naive Tregs and CAR memory Tregs (Figures S4F–S4H). However, CAR memory Tregs had a slight yet statistically significant increase in the frequency of $FOXP3^-$ $HELIOS^-$ cells post-CAR stimulation compared with CAR naive Tregs (Figure S4I). Intriguingly, while naive CAR Tregs suppressed $CD4^+$ and $CD8^+$ Tresp proliferation more effectively than memory CAR Tregs (Figures S5A and S5B), memory CAR Tregs downregulated CD80 surface expression on target cells to a larger extent than naive CAR Tregs (Figure S5C). Of note, both CAR naive Tregs and CAR memory Tregs secreted higher levels of inflammatory cytokines and chemokines than TCRCD28-activated Tregs, with no clear trend between the two CAR Treg subsets: CAR naive Tregs secreted significantly more TNF-α, TNF-β, IL-3, and M-CSF, yet less IL-17A, IL-6, and G-CSF than CAR memory Tregs (Figure S5D). Importantly, both CAR naive Tregs and CAR memory Tregs secreted similarly high amounts of IFN-γ across three donors, while Tregs activated via endogenous TCR/CD28 secreted negligible levels of IFN-γ (Figure S5D). Therefore, starting CAR Treg manufacture by FACS sorting $CD45RA^+CD45RO^-$ naive Tregs, excluding $CD45RA^-CD45RO^+$ memory Tregs, does not prevent inflammatory cytokine secretion by CAR Tregs, with naive and memory Treg subsets having equal capacity and propensity to secrete IFN-γ upon CAR stimulation.

### Lowering CAR affinity reduces inflammatory cytokine production by CAR Tregs

T cell activation and function are influenced by the affinity of the TCR and the strength of costimulation.[74,75] Moreover, as mentioned previously, Tregs exhibit dampened activation of several pathways downstream of TCR signaling.[33,34] Inspired by these notions, we modified our CAR construct to dissect which of its features was responsible for the proinflammatory shift observed in CAR-activated Tregs and potentially better mimic endogenous TCR/CD28 engagement in Tregs. To reduce affinity, we modified the extracellular domain of the CAR by swapping the FMC63 scFv domain with an scFv sequence, CAT-13.1E10, which binds to the same CD19 residues as FMC63 but with a 40-fold lower affinity.[76] To reduce costimulation strength, we modified the intracellular domain of the CAR by mutating all tyrosines of the CD28 signaling domain, as well as both prolines of its PYAP domain, which binds to LCK.[30,77] We then introduced these two new CARs, which we called CAT and PY3, respectively, into freshly isolated Tregs (Figures S6A and S6B) to investigate the impact of affinity and costimulation strength on CAR Tregs. We activated CAR, CAT, and PY3 Tregs via the CAR with irradiated CD19-K562 cells (in parallel with TCR/CD28 activation and no activation) and performed whole-transcriptome RNA-seq as described earlier. We found that CAR, CAT, and PY3 Tregs clustered together and TCR and No Act Tregs clustered together based on gene expression (Figure S6C), indicating that, at the whole-transcriptome level, activation via a lower-affinity CAR or a lower-signal 2 strength CAR remain more akin to CAR activation than to endogenous TCR/CD28 activation. Nevertheless, looking at the genes uniquely upregulated by each of these four modes of activation (TCR, CAR, CAT, PY3) revealed that CAR Tregs uniquely upregulated more genes (1,394) than any of the other conditions (Figure S6D). Focusing on CAT Tregs and PY3 Tregs, we found that, despite a large overlap in upregulated genes between these two conditions (Figure S6E), PY3 Tregs uniquely upregulated the inflammatory genes *IL17A*, *IL1B*, *CXCL11*, *CSF3*, and, importantly, *CD40LG*, as well as the cytotoxicity genes *GZMB*, *CRTAM*, and *NKG7* (Table S8). Indeed, PY3 Tregs had *IL17A*, *IFNG*, *CD40LG*, and *GZMB* expression levels almost as high as CAR Tregs, whereas CAT Tregs had expression levels of these same genes almost as low as TCR/CD28-activated Tregs (Figure S6F). Interestingly, however, both CAT and PY3 Tregs still had *CCR2*, *CCR5*, and *CXCR3* expression levels as low as CAR Tregs, suggesting that lower affinity (CAT) and lower costimulation strength (PY3) did not rescue expression of these chemokine receptor genes to the levels observed in TCR/CD28-activated Tregs (Figure S6F). Altogether, activation via the lower-affinity CAT construct, but not via the lower-costimulation strength PY3, resulted in visibly lower expression of inflammatory genes, kindling our interest in further comparing the CAR and CAT constructs head-to-head. CAR and CAT Tregs both displayed robust receptor surface expression post-$GFP^+$ cell sorting, based on Myc-tag expression (Figures 6A and S6A). Activated CAR Tregs and CAT Tregs had

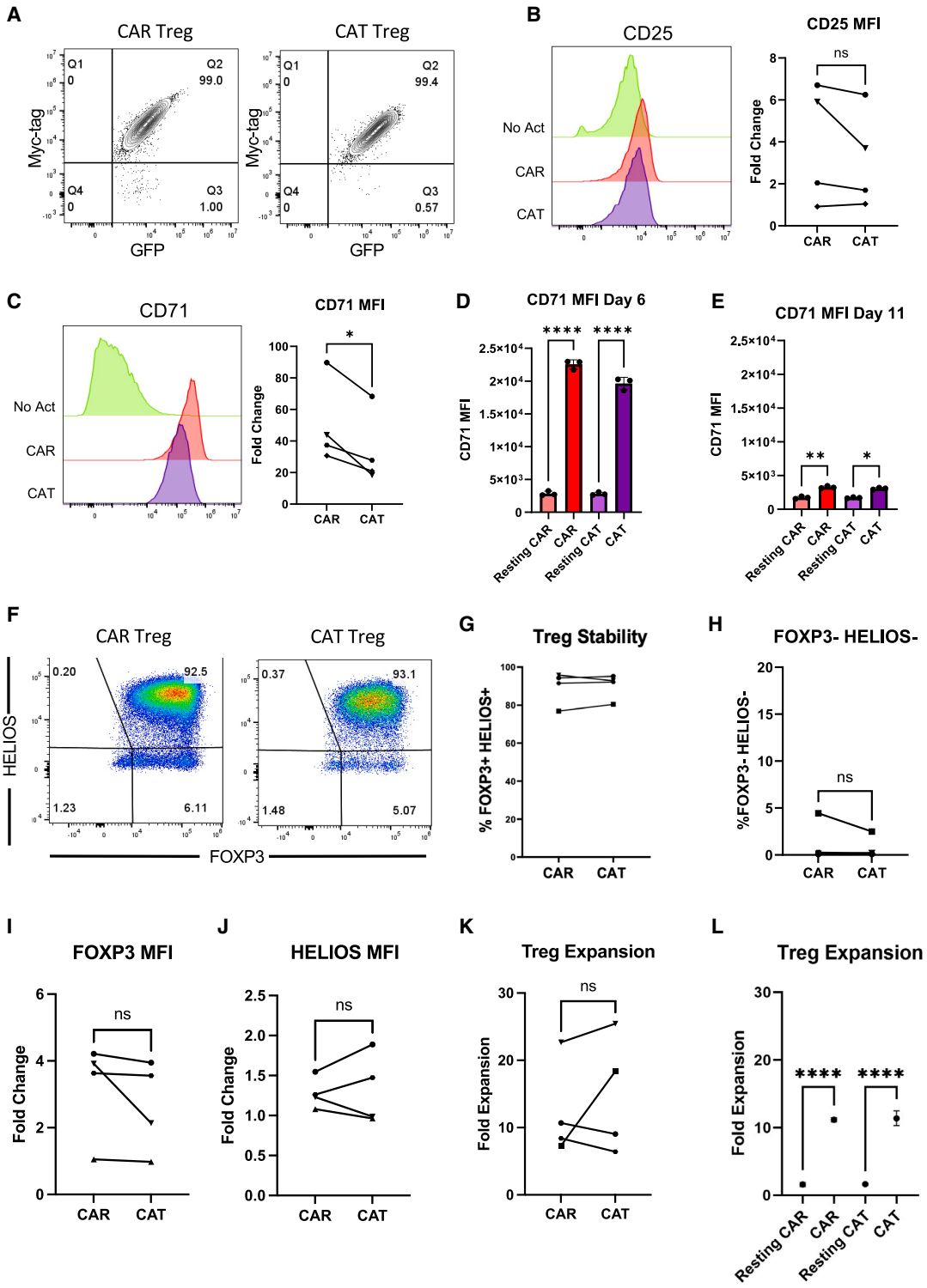


**Figure 6. Lowering CAR affinity reduces the extent of CAR Treg activation**

(A) Representative contour plot of surface expression (Myc-tag) of high-affinity FMC63 CD19 CAR (CAR) and low-affinity CAT-13.1E10 CD19 CAR (CAT) in Tregs. (B) CD25 surface expression 48 h after Treg activation. Representative histograms on the left and summary data across donors of fold change in CD25 mean fluorescence intensity (MFI) in relation to No Act Tregs on the right. (C) CD71 surface expression 48 h after Treg activation. Representative histograms on the left and summary data across donors of

*(legend continued on next page)*

similar upregulation of CD25 (Figure 6B), yet CAT Tregs upregulated CD71 to a smaller extent than CAR Tregs (Figure 6C). To validate that our new CAR construct did not induce tonic signaling, we evaluated CD71 expression in CAR Tregs and CAT Tregs over time following activation with irradiated CD19-K562 cells and compared with cells that were not activated (resting). These experiments revealed that CD71 is never induced in the resting engineered Tregs, while the activated CAR and CAT Tregs lose CD71 expression over time, resembling a normal T cell activation cycle (Figures 6D and 6E). In addition, activated CAR Tregs and CAT Tregs had an equally stable Treg phenotype based on similar levels of FOXP3 and HELIOS (Figures 6F–6J) expression. Moreover, CAR Tregs and CAT Tregs expanded to a similar extent post-activation with irradiated CD19-K562 cells (Figure 6K), while CAR and CAT Tregs co-cultured with control irradiated K562 did not expand, another line of evidence of the absence of tonic signaling (Figure 6L) At the functional level, CAT Tregs were superior at suppressing $CD4^+$ T cells (Figure 7A), but not $CD8^+$ T cells (Figure 7B), downregulated CD80 surface expression on target cells to a larger extent (Figure 7C), and were less cytotoxic toward NALM6 cells (Figure 7D) than CAR Tregs. Moreover, CAT Tregs secreted sCD40L, IFN-γ, TNF-α, and IL-17A (Figure 7E), as well as IL-3, IL-4, and IL-6 (Figure S7) at the same low levels as TCR/CD28-activated Tregs. Altogether, reducing the affinity of the CAR construct by 40-fold resulted in engineered Tregs with higher suppressive capacity, lower cytotoxic activity, and reduced inflammatory cytokine secretion.

Next, we sought to explore whether measuring the levels of the surface markers CD40L and TIGIT could help identify proinflammatory CAR Tregs and how these levels were affected by the affinity of the CAR. We activated TCR, CAR, and CAT Tregs with the respective irradiated K562 cell lines overnight and, following a 5-h treatment with brefeldin A, performed surface staining for CD40L and TIGIT, and then intracellular staining for IFN-γ. While CAR Tregs and CAT Tregs both had higher expression of CD40L than TCR/CD28-activated Tregs (Figure 8A), CAT Tregs had TIGIT levels almost as high as TCR/CD28-activated Tregs (Figure 8B). Co-expression analysis revealed that, while the majority of TCR Tregs and CAT Tregs were $TIGIT^+CD40L^{low}$ cells, CAR Tregs were mostly TIGIT negative, with 20% of the cells being $TIGIT^-CD40L^{hi}$ cells (Figure 8C). Across the four subpopulations of CD40L and TIGIT expression combinations, high expression of CD40L correlated with high IFN-γ production, with 20% of $CD40L^{hi}$ CAR Tregs producing IFN-γ vs. only 5% of $CD40L^{low}$ CAR Tregs (Figure 8D). Hence, CD40L surface expression correlates with IFN-γ production in Tregs. Still, IFN-γ-producing TCR Tregs and CAT Tregs were significantly less abundant than IFN-γ-producing CAR Tregs irrespective of CD40L expression (Figure 8D), indicating that there are additional differences between $CD40L^{hi}$ high-affinity CAR-activated Tregs and $CD40L^{hi}$ TCR/CD28-activated or low-affinity CAR-activated Tregs.

## DISCUSSION

The application of CAR technology to Tregs to induce or re-establish immune tolerance has been met with cautious optimism. While CAR-engineered Tregs have shown promising results *in vitro* and in murine disease models of GvHD and skin graft rejection,[15–18] their suboptimal efficacy in preclinical models of vascularized organ transplantation and autoimmune disease,[20,23,24] settings where antigen-specific TCR Tregs have demonstrated efficacy in reversing disease,[26,78] exposes the current limitations of CAR Treg-based strategies. This disparity underscores the need for a more complete understanding of how CAR Tregs function at a molecular level compared with their endogenous TCR/CD28 activated counterparts.

Here, we utilized a well-established CAR with a CD28-CD3ζ signaling domain with the goal of comparing TCR/CD3 and CD28 signaling delivered via a CAR and via the endogenous TCR/CD3 complex and the CD28 receptor, with the activating signals being provided by target cells, not antigen-coated beads, for both modes of activation. Our rationale for this comparative investigation is rooted in the fact that CAR constructs were originally designed and optimized for proinflammatory cytotoxic T cells. Consequently, we hypothesized that applying this same CAR architecture to immunosuppressive Tregs does not fully elicit or even disrupts Treg function, potentially jeopardizing their safe and effective clinical application.

On a first look, CAR- and TCR/CD28-activated Tregs were similar in terms of activation marker upregulation, expansion, and, importantly, stability, as there were no differences in the percentage of $FOXP3^+HELIOS^+$ or $FOXP3^-HELIOS^-$ cells between TCR/CD28-activated and CAR-activated Tregs (Figure 1). Hence, functional differences between CAR- and TCR/CD28-activated Treg populations due to Tregs losing FOXP3 expression or selective expansion of contaminating Teff cells could be ruled out. CAR Tregs, however, had lower CD25 levels across all donors (Figure 1C). This observation foreshadowed our findings that CAR Tregs were inferior at suppressing the proliferation of $CD4^+$ T cells and $CD8^+$ T cells (Figures 2A and 2B), an activity known to be dependent on IL-2 deprivation.[79] CAR

fold change in CD71 MFI in relation to No Act Tregs on the right. (D) CD71 surface expression on non-activated CAR Tregs (Resting CAR), activated CAR Tregs (CAR), non-activated CAT Tregs (Resting CAT), and activated CAT Tregs (CAT) 6 days post-activation. (E) CD71 surface expression on resting CAR, CAR, resting CAT, and CAT Tregs 11 days post-activation. (F) Representative dot plots of FOXP3 and HELIOS expression in CAR Tregs and CAT Tregs. (G) Percentage of $FOXP3^+HELIOS^+$ cells in CAR Tregs and CAT Tregs across donors. (H) Percentage of $FOXP3^-HELIOS^-$ cells in CAR Tregs and CAT Tregs across donors. (I) Fold change in FOXP3 MFI in CAR Tregs and TCR Tregs over No Act Tregs across donors. (J) Fold change in HELIOS MFI in CAR Tregs and CAT Tregs over No Act Tregs across donors. (K) Fold expansion in cell number for CAR Tregs and CAT Tregs 1 week post-activation. (L) Fold expansion in cell number for resting CAR, CAR, resting CAT, and CAT Tregs 1 week post-activation. For (B and C) and (H–K), values are the mean of technical triplicates per blood donor ($n = 4$), with lines collecting the data points from the same donor and paired Student's t test was used to assess statistical significance. For (D), (E), and (L), values represent technical replicates of representative experiment and one-way ANOVA with Tukey's multiple comparison correction was used to assess statistical significance. $^{****}p < 0.0001$, $^{***}p < 0.001$, $^{**}p < 0.01$, $^{*}p < 0.05$; ns, not significant.

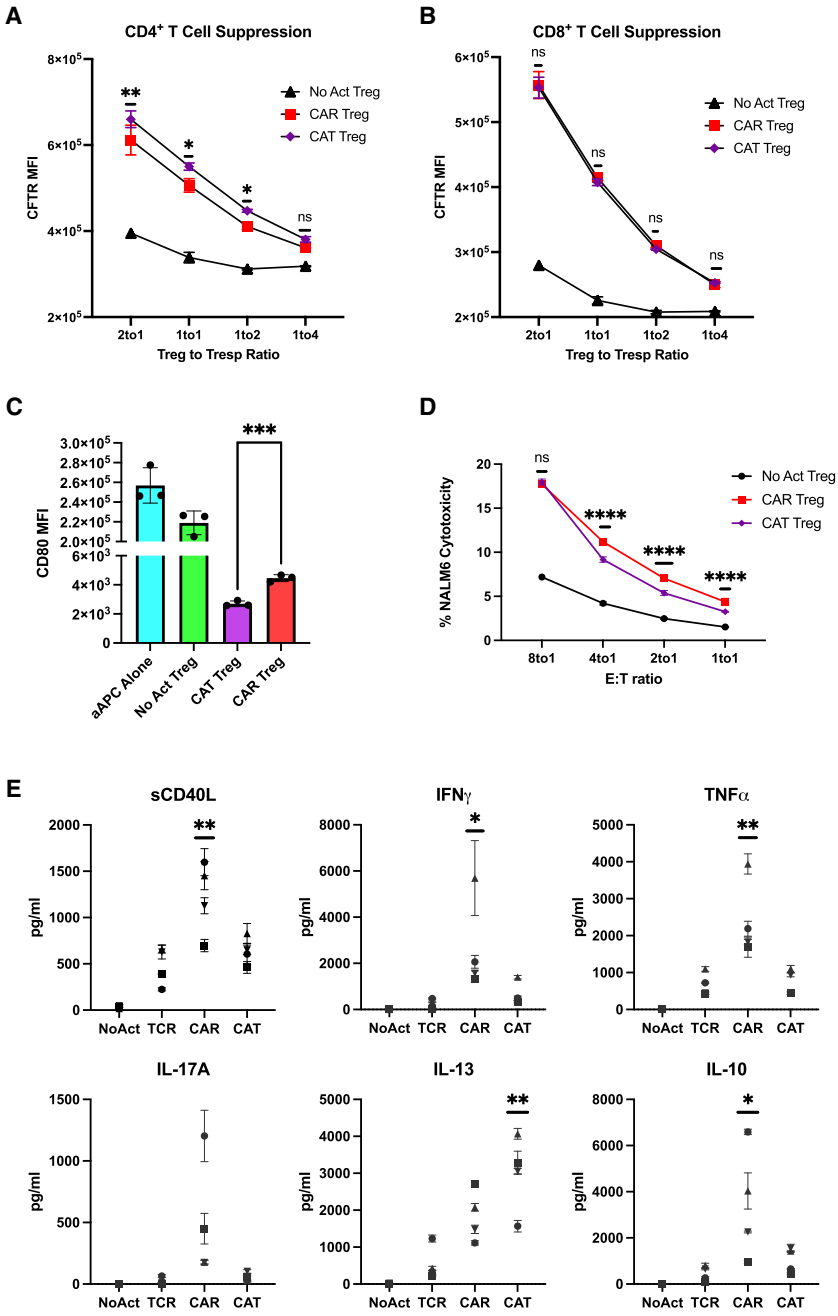


**Figure 7. Lowering CAR affinity improves CAR Treg suppressive function**

(A) Inhibition of CellTrace Far Red (CTFR)-labeled CD4+ T responder cell (Tresp) proliferation by Tregs. (B) Inhibition of CTFR-labeled CD8+ Tresp proliferation by Tregs. (C) Downregulation of CD80 surface expression in CD80-CD64 NALM6 cells (aAPC, artificial antigen-presenting cells) by Tregs. (D) Treg cytotoxicity toward target NALM6 cells at different effector to target E:T ratios. (E) Levels of cytokines secreted by No Act Tregs, TCR Tregs, CAR Tregs, and CAT Tregs 48 h post-activation. For (A)–(D), values represent technical replicates of representative experiment. Bars represent mean ± SD. Statistical significance was determined using two-way ANOVA with Tukey's multiple comparison correction (A, B, and D) or unpaired Student's t test (C). For (E), values represent mean ± standard deviation (SD) of technical triplicates per blood donor ($n = 4$) and one-way ANOVA test with Tukey's multiple comparison correction was used to determine statistical significance. ****$p < 0.0001$, ***$p < 0.001$, **$p < 0.01$, *$p < 0.05$; ns, not significant.

Tregs were also inferior at downregulating CD80 expression on target cells (Figure 2C), another important Treg suppression mechanism. Of note, CTLA4 was not differentially expressed between CAR Tregs and TCR Tregs, as determined by RNA-seq (Table S5).

Of note, CAR Tregs were not cytotoxic toward CD19-expressing A549 cells (Figure S2F), engineered lung epithelial cancer cells, lending hope that CAR Tregs might not be directly cytotoxic toward non-immune tissues and organs. This possibility deserves special consideration, as CAR Tregs currently in clinical trials (NCT05234190) target HLA-A2 expressed specifically in the transplanted organ to be protected from immune rejection.[29]

Our functional assays suggested that CAR activation causes a shift from suppression to cytotoxicity (Figure 2). In line with this notion, CAR Tregs preferentially upregulated Teff cell inflammatory gene pathways (Figure 3) and uniquely produced inflammatory cytokines, notably IFN-γ (Figures 4A, 4B, and S3B). IFN-γ is an unwanted cytokine in the context of CAR Treg-based therapy, as it can lead to innate immune cell activation and HLA upregulation,[80] thus being counterproductive in autoimmunity and organ transplant rejection. CAR Tregs did not, however, produce IL-2 (Figure 4C), cementing the idea that CAR Tregs remain stable Tregs upon activation. Lack of IL-2 production is a hallmark of Treg identity, with FOXP3 directly inhibiting transcription of the IL-2 gene.[81] Curiously, IFN-γ-producing FOXP3+ Tregs have been described previously in autoimmunity and in solid tumors,[41,82] suggesting that high-affinity CAR activation may be tapping into Treg plasticity to elicit inflammatory cytokine production. CAR Teff cells also produced more IFN-γ than TCR Teff cells (Figures 4A and 4B), suggesting that some aspect of high-affinity CAR activation induces high IFN-γ production across cell subsets. Previous reports have described the emergence of T helper-like Tregs that share transcription factor and chemokine gene expression patterns with T helper genes, e.g., Th1-like Tregs that express T-BET and CXCR3.[83] Yet, we did not find CAR activation to

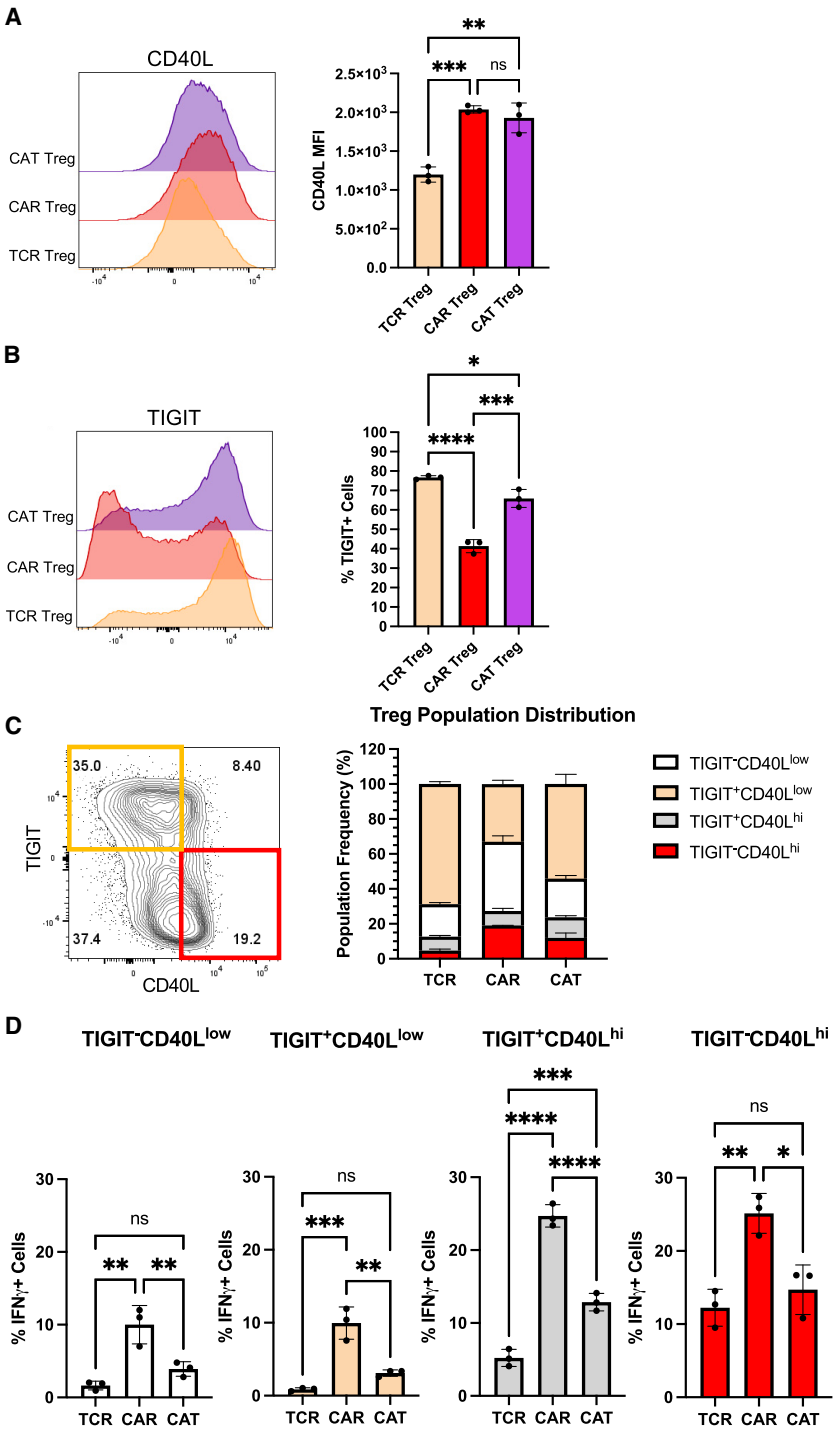


**Figure 8. CD40L expression is associated with IFN-γ production in CAR Tregs**

(A) CD40L surface expression in TCR Tregs, CAR Tregs, and CAT Tregs 18 h post-activation. Representative histograms on the left and summary data on the right. (B) TIGIT surface expression in TCR Tregs, CAR Tregs, and CAT Tregs 18 h post-activation. Representative histograms on the left and summary data on the right. (C) Relative frequency of TIGIT$^{-}$CD40L$^{low}$, TIGIT$^{+}$CD40L$^{low}$, TIGIT$^{-}$CD40L$^{hi}$, and TIGIT$^{+}$CD40L$^{hi}$ cells among TCR Tregs, CAR Tregs, and CAT Tregs 18 h post-activation. (D) Frequency of IFN-γ-producing cells among TIGIT$^{-}$CD40L$^{low}$, TIGIT$^{+}$CD40L$^{low}$, TIGIT$^{-}$CD40L$^{hi}$, and TIGIT$^{+}$CD40L$^{hi}$ subpopulations for TCR Tregs, CAR Tregs, and CAT Tregs 18 h post-activation. For (A), (B), and (D), values represent technical replicates of representative experiment. Bars represent mean ± standard deviation (SD). Statistical significance was assessed using one-way ANOVA test with Tukey's multiple comparison correction. $^{****}p < 0.0001$, $^{***}p < 0.001$, $^{**}p < 0.01$, $^{*}p < 0.05$; ns, not significant.

upregulate expression of TBX21, the gene coding for T-BET, in CAR Tregs at the bulk level, in spite of a 40-fold increase in IFNG expression (Figure 5C). Future profiling of gene expression at the single-cell level, as well as gene overexpression and deletion experiments, are poised to elucidate the gene circuitry conferring subpopulations of CAR Tregs partial Teff cell gene expression and exuberant cytokine and chemokine production.

Intriguingly, our study also identified heightened expression of CD40L in CAR Tregs (Figure 5), correlating with IFN-γ expression (Figure 8). Activated CD4$^{+}$ T helper cells express CD40L, which binds to CD40 on the surface of B cells; CD40L-CD40 signaling is required for high-titer high-affinity class-switched antibody production by B cells and for humoral memory formation.[61] Tregs, in contrast, do not typically express CD40L, with CD40L negativity having been put forward previously as a strategy to isolate activated Tregs.[84,85] While the implications of this *de novo* expression of CD40L in Tregs are not explored in this study, they warrant further investigation, possibly including unwanted activation of CD40-expressing B cells and macrophages and concomitantly tissue damage.[86] Of note, CD40L provides a potential surface marker to further purify and interrogate proinflammatory CAR Tregs in future studies.

Recent studies have used specifically CD45RA$^{+}$ naive Tregs as their starting Treg population before genetic engineering to minimize the potential for Treg destabilization,[69,72] prompting us to investigate whether this strategy would mitigate the proinflammatory Treg phenotype induced by CAR activation. We found that, starting with either CD45RA$^{+}$ naive or CD45RO$^{+}$ memory Tregs, did not lead to differences in CAR Treg CD40L expression (Figure S4) or IFN-γ secretion (Figure S5), indicating that removing CD45RO$^{+}$ memory Tregs during the initial Treg FACS sort has no

impact on the inflammatory profile of CAR Tregs and further strengthening our hypothesis that CAR activation confers Teff cell properties to bona fide Tregs.

On the other hand, lowering CAR affinity by swapping the FMC63 scFv with the lower-affinity CAT13.1E10 (CAT) scFv[76] resulted in Tregs with a phenotype closer to that of TCR/CD28-activated Tregs, namely lower IFN-γ production (Figures 7E and 8), higher TIGIT expression (Figure 8B), and a lower frequency of CD40L-expressing cells (Figure 8). CAT Tregs also displayed higher suppression of $CD4^+$ T cell proliferation, a greater downregulation of CD80 expression on target cells, and lower cytotoxicity toward NALM6 than CAR Tregs (Figure 7), establishing scFv affinity as a key parameter in CAR design for Tregs. Nevertheless, some differences between CAT Tregs and TCR Tregs subsisted, namely low expression of some chemokine receptor genes, such as CCR2 and CCR5, previously shown to be key to Treg trafficking,[87] and slightly higher secretion of select cytokines (Figures 7E, S6, and S7). Of note, neither CAR nor CAT expression resulted in tonic signaling (Figures 6D, 6E, and 6L).

Interestingly, CAR Tregs were slightly more cytotoxic toward target NALM6 cells than CAT Tregs (Figure 7D). This could be due to the marked difference in affinity between the CAR (FMC63) and the CAT (CAT-13.1E10) scFv (Figure S8). More specifically, the difference in cytotoxicity could be due to the CAR being slower at dissociating from its antigen than CAT. The dissociation constant $K_D$, which is inversely proportional to the binding affinity, for the FMC63 CD19 CAR is $3.3 \times 10^{-10}$ M, approximately 40-fold lower than the CAT-13.1E10 CD19 CAR $K_D$ of $1.4 \times 10^{-8}$ M.[76] Reported $K_D$ values for CARs are in the range of $10^{-7}$ to $10^{-10}$ M [88] In contrast, the $K_D$ of a human TCR is normally in the lower range of $10^{-4}$ to $10^{-6}$ M [74,89,90] (Figure S8). The $K_D$ for a receptor is the ratio between how fast the receptor dissociates from its antigen, $k_{off}$, and how fast the receptor binds to its antigen, $k_{on}$. Seminal work showed that the longer a Treg is bound to a target DC, the more likely the Treg is to kill that cell.[49] Indeed, residence time ($t_{1/2} = \ln 2/k_{off}$) of the FMC63 CAR is a staggering 3 h,[76,90] while the $t_{1/2}$ of CAT-13.1E10 CAR is 4 min. In comparison, a typical human TCR has a $t_{1/2}$ of 4 s (Figure S8). Hence, the increased toxicity of CAR Tregs could be due to increased time bound to the target cells.

While our study finds a clear unique phenotype in high-affinity CAR-activated Tregs in comparison with endogenous TCR/CD28-activated Tregs and low-affinity CAR-activated Tregs, only three CAR constructs specific for one target were used in this study. Further investigations are needed with different CAR constructs to cover a wider range of affinities, as well as a diversity of targets, as target molecule density on target cells has also been shown to influence CAR T cell function.[91] Moreover, some parameters of CAR constructs, such as the hinge and transmembrane domains,[91,92] as well as alternative signaling domains,[47,93] were not explored in this study and may yield further insight. Of note, we utilized target cells decorated with anti-CD3 antibody and expressing CD80 with the goal of stimulating the endogenous TCRs and the endogenous CD28 receptor of all Tregs in the population. Transducing Tregs with different MHC class II restricted individual TCRs,[94] each with a different affinity, and activating them with APCs presenting their respective cognate peptide-MHC complexes in parallel will better represent the TCR immune synapse and hence holds the potential to confirm and expand the observations of this study. Another limitation of this study resides in the fact that it does not fully unveil the molecular mediators responsible for the induction of a proinflammatory phenotype and gene signature in Tregs by high-affinity CAR activation. Finally, this study does not dissect the consequences of the unique CAR Treg phenotype discovered here *in vivo*, such as the effect of CAR Treg-derived IFN-γ on a local milieu or the impact of CD40L-CD40 signaling on CAR Tregs and surrounding immune cells. Experiments using human CAR Tregs in humanized mouse models and murine CAR Tregs in immunocompetent mouse models will shed light on these important aspects.

The speed of translating Tregs to the clinic has been vertiginous, with only 10 years elapsing from their identification in humans in 2001 to their testing in GvHD patients in 2011.[5] Yet, CAR Tregs are in their infancy as a strategy for immune regulation. Our work indicates that CAR Tregs can have a dual nature–proinflammatory yet still retaining key immunosuppressive features–calling for a more nuanced understanding of their complex signaling and functional outcomes if CAR Tregs are to become a safe and efficacious therapeutic modality. It also emphasizes how important it will be to tailor CAR constructs to Treg biology. Our data suggest that one possible avenue to achieve this is to ensure that the CAR affinity is not too high, lest it bestow Tregs with undesired inflammatory properties.

## MATERIALS AND METHODS

### Molecular biology

CD64-2A-CD80, $CD19_{ECD}$-$PDGFR_{TM}$, and CD19CAR-2A-GFP lentiviral plasmids were synthesized by VectorBuilder (Chicago, IL). All genes were driven by an EF1A promoter. The CD19 CAR genes contained a CD8a signal peptide, an N-terminal Myc-tag, a scFv sequence recognizing human CD19, a CD8 hinge domain, a CD28 transmembrane domain, and a CD28-CD3ζ signaling domain. The high-affinity anti-CD19 scFv sequence (FMC63) in the CAR CD19CAR construct was obtained from Bloemberg et al.,[35] the mutated CD28 signaling domain in the "PY3" CD19CAR construct was obtained from Salter et al.,[77] and the low-affinity anti-CD19 scFv sequence (CAT-13.1E10) in the "CAT" CD19CAR construct was obtained from Ghorashian et al.[76] Lentivirus particles were produced by VectorBuilder and shipped to the laboratory, where they were stored in aliquots at −80°C until use. Construct sequences are available in Table S11. The high-affinity FMC63 CD19 CAR 2A GFP (CAR), the low-affinity CAT-13.1E10 CD19 CAR 2A GFP (CAT), and the lower-signaling strength FMC63 CD19 mutant CD28 CAR 2A GFP (PY3) lentiviral plasmids have been deposited on Addgene.

### Regulatory T cell isolation

Human peripheral blood leukopaks from de-identified healthy donors were purchased from STEMCELL Technologies (Vancouver,

Canada). $CD4^+$ T cells and $CD8^+$ T cells were enriched using the EasySep Human $CD4^+$ T cell Isolation Kit and EasySep Human $CD8^+$ T cell Isolation Kit (STEMCELL Technologies), respectively, as per manufacturer's instructions. Enriched $CD4^+$ T cells were then stained for CD4, CD25, and CD127, and $CD4^+CD25^{hi}CD127^{low}$ regulatory T cells (Tregs), previously shown to be bona fide Tregs,[36,37] and $CD4^+CD25^{low}CD127^{hi}$ effector T (Teff) cells were purified by FACS using a BD FACS Aria II Cell Sorter (Beckton Dickinson, Franklin Lakes, NJ). Post-sort analyses confirmed greater than 95% purity. T cells were activated with anti-CD3/CD28 beads (Gibco, Thermo Fisher Scientific) at a 1:1 ratio and recombinant human IL-2 (PeproTech, Thermo Fisher Scientific), and expanded in RPMI-1640 medium supplemented with 10% fetal bovine serum, glutamax, penicillin-streptomycin, HEPES, non-essential amino acids, and sodium pyruvate (all from Gibco, Thermo Fisher Scientific). Tregs were cultured with 1,000 IU/mL IL-2, $CD4^+$ Teff cells with 100 IU/mL IL-2, and $CD8^+$ T cells with 300 IU/mL IL-2.[45] Antibodies used for FACS and flow cytometry can be found in Table S9.

#### T cell transduction and expansion

Two days after activation, T cells were transduced with CAR lentivirus at a multiplicity of infection of 1 (one particle per cell) in the presence of IL-2. After adding the lentivirus, T cells were centrifuged at 1,000 × *g* at 32°C for 1 h. Following transduction, T cells were maintained and expanded in RPMI-10 medium with fresh medium and IL-2 being given every 2 days. CAR-expressing T cells were FACS sorted based on reporter GFP expression.

#### CAR Treg activation, stability, and expansion

CAR Tregs were co-cultured with irradiated K562 (No Activation), CD19-expressing K562 (CAR Activation), or CD64-and CD80-expressing K562 previously loaded with anti-CD3 antibody (OKT3, BioLegend, San Diego, CA) at 1 μg/mL for 1 h[38] (TCR/CD28 Activation) at a 1:1 ratio of CAR Tregs to K562 cells in RPMI-10 medium supplemented with 1,000 IU/mL IL-2. Surface expression of CD71 and CD25 (Activation) was assessed at 48 h by flow cytometry. Parallel co-cultures were kept for 8 days to assess expression of FOXP3 and HELIOS (Stability) by intracellular staining using the FOXP3/Transcription Factor Staining Buffer Set (eBioscience, Thermo Fisher Scientific), according to the manufacturer's instructions. Cell numbers were also assessed at this time (Expansion). Flow cytometry data were acquired in a five-laser Beckman Coulter CytoFLEX flow cytometer or a three-laser Cytek Northern Lights spectral flow cytometer. FlowJo v.10.9 software (BD Life Sciences, Franklin Lakes, NJ) was used for flow cytometry data analysis.

#### T cell suppression assay

CAR Tregs were activated via CAR (with irradiated CD19-K562 cells), via TCR/CD28 (with irradiated CD64-CD80-K562 cells loaded with anti-CD3 OKT3 antibody), or left resting (with irradiated K562 cells) at a 1:1 Treg to target cell ratio in round-bottom 96-well plates. In parallel, $CD4^+$ and $CD8^+$ Tresp cells were mixed at a 1:1 ratio, labeled with CellTrace Violet (CTV) or CellTrace Far Red (CTFR) according to the manufacturer's instructions (Invitrogen, Thermo Fisher Scientific), and activated with anti-CD3/CD28 beads at a 1:5 bead to cell ratio overnight.[45,95] The following day, Tresp cells were first debeaded and then co-incubated with activated Tregs in round-bottom 96-well plates at different Treg:Tresp ratios for 3 days in the absence of exogenous IL-2.[45,95] Co-cultures were then harvested, stained for CD4 and CD8, and CTV or CTFR dye dilution measured via flow cytometry.

#### Artificial APC suppression assay

$CAR^+$ Tregs were incubated with CD64-CD80-NALM6 cells (CAR activation) and $CAR^-$ Tregs were incubated with CD64-CD80-NALM6 loaded with anti-CD3 (TCR/CD28 activation) for 4 days. Co-cultures were then harvested and CD80 surface expression ssessed using flow cytometry.

#### Cytotoxicity assay

$CAR^+$ Tregs or $CAR^+$ Teff cells were incubated with NALM6 cells and $CAR^-$ Tregs or $CAR^-$ Teff cells were incubated with CD64-CD80-NALM6 cells loaded with anti-CD3 (OKT3 antibody) at different E:T ratios for 24 h. Alternatively, $CAR^+$ Tregs or $CAR^+$ Teff cells were incubated with CD19-A549 cells. Target cell killing was then assessed using the CyQUANT Cytotoxicity Lactate Dehydrogenase Release (a measure of cell death) Assay kit (Thermo Fisher Scientific) as per the manufacturer's instructions.

#### CRISPR-Cas9 gene editing

Two days after activation with anti-CD3/28 beads and 1,000 IU/mL IL-2, Tregs were debeaded and electroporated with Cas9 (TrueCut v.2, Thermo Fisher Scientific) and guide RNA (Synthego, Redwood City, CA) ribonucleoprotein complexes using a Neon system (Thermo Fisher Scientific) with settings 2,200 V, 20 ms, 1 pulse. Electroporated cells were recovered in antibiotic-free RPMI-10 with IL-2 and expanded until analysis. The guide RNA sequence used to target the *PRF1* gene (encoding the perforin protein) was 5′-CCTTCC CAGTGGACACACAA-3′. Control WT cells were electroporated with Cas9 alone. CRISPR-Cas9 genome editing efficiency was assessed by PCR amplification of a 500 bp region of the genomic DNA containing the *PRF1* gRNA cutting site, using the forward primer 5′-AAGGGAGCAGTCATCCTCCA-3′ and the reverse primer 5′-CATTGCTGGTGGGCTTAGGA-3′, followed by Sanger sequencing (Eurofins Genomics, Louisville, KY) and sequence analysis using TIDE (https://tide.nki.nl/) to obtain indel frequency.

#### Whole-transcriptome RNA-seq analysis

CAR Tregs and CAR Teff cells were co-cultured with irradiated K562 (No Activation), CD19-K562 (CAR Activation), or CD64-CD80-K562 loaded with anti-CD3 antibody (TCR/CD28 Activation) at a 1:1 ratio in RPMI-10 medium. CAR Treg co-cultures were supplemented with 1,000 IU/mL IL-2. After 24 h, $CD4^+$ cells were isolated using the EasySep Human CD4 Positive Selection Kit (STEMCELL Technologies), following the manufacturer's instructions. RNA-seq libraries were built using poly(A) selection and paired-end sequencing was performed with the Illumina NovaSeq 6000 platform. For data analysis, FastQC was first applied to assess the quality of raw

sequencing reads. Alignment was then performed with Spliced Transcripts Alignment to a Reference alignment software[96] using the most recent build of the human GENCODE reference genome (release 44, GRCh38.p14). Next, Samtools were employed for filtering and sorting uniquely aligned reads and FeatureCounts for annotating and quantifying raw gene counts.[97] Gene transfer format files for gene annotation from GENCODE (hg38/GRCh38) were then obtained. DESeq2[98] was used for normalization and downstream differential gene expression analysis. Genes showing a false discovery rate <0.05 and absolute $\log_2$ fold change >1 in magnitude were considered differentially expressed in pairwise comparisons. The topmost significantly differentially upregulated genes were used for GSEA. Some RNA-seq data inspection and visualization was performed with the help of Venny 2.0 (https://bioinfogp.cnb.csic.es/tools/venny/index2.0.2.html) and iDEP 2.0[99] (http://bioinformatics.sdstate.edu/idep/). Raw and processed data to support the findings of this study have been deposited in GEO under accession number GSE282623. Code used to analyze the RNA-seq data in this paper can be found at https://github.com/BioinformaticsMUSC/Ferreira_High_Affinity_CAR_Treg.

### Cytokine secretion

Supernatants from Treg and Teff cell co-cultures with K562 target cell lines were collected, stored at −80°C and shipped to EveTech (Calgary, Canada) for cytokine quantitation using multiplex ELISA.

### Intracellular cytokine production

CAR Tregs and CAR Teff cells were activated overnight via CAR (with irradiated CD19-K562 cells), via TCR/CD28 (with irradiated CD64-CD80-K562 cells loaded with anti-CD3 antibody), or left resting (with irradiated K562 cells) at a 1:1 Treg to target cell ratio in round-bottom 96-well plates. The following day, co-cultures were treated with brefeldin A (BioLegend) for 5 h and harvested for intracellular cytokine staining with the FOXP3/Transcription Factor Staining Buffer Set (eBioscience, Thermo Fisher Scientific), according to the manufacturer's instructions.

### qPCR

Total RNA from CAR and TCR/CD28 activated Tregs 24 h post-activation was isolated using TRIzol (Thermo Fisher Scientific), according to the manufacturer's instructions. A total of 1,000 ng of RNA was used for cDNA synthesis with the High-Capacity cDNA Reverse Transcription Kit (Bio-Rad, Hercules, CA). Real-time PCR was performed with iTaq Universal SYBR Green Supermix (Bio-Rad) on a Bio-Rad Real-time System C1000 Thermal Cycler. Target gene Ct values were normalized to RPL13A Ct value. Sequences of the primers used for qPCR can be found in Table S10.

### Statistics

Statistical analyses were performed using GraphPad Prism v.10.0.0 (GraphPad Software, La Jolla, CA).

## DATA AND CODE AVAILABILITY

All data in this article are available upon request to the corresponding author (L.M.R.F.). RNA-seq data have been deposited online with GEO number xxx and the code used to analyze the RNA-seq data is available online at xxx. Sequences for all constructs used in this study are provided in Table S11 and CAR constructs have been deposited on Addgene.

## ACKNOWLEDGMENTS

This work was supported by Medical University of South Carolina and Hollings Cancer Center startup funds, Human Islet Research Network Emerging Leader in Type 1 Diabetes grant U24DK104162-07, American Cancer Society Institutional Research Grant IRG-19-137-20, Diabetes Research Connection grant IPF 22-1224, and Swim Across America grant 23-1579 to L.M.R.F., and Cellular, Biochemical and Molecular Sciences training grant 5T32GM132055 and Hollings Cancer Center Lowvelo Graduate Fellowship to R.W.C. Supported in part by the Flow Cytometry and Cell Sorting Shared Resource, Hollings Cancer Center, MUSC (P30 CA138313) and the CCND Genomics and Bioinformatics Core, MUSC (P20 GM148302). We thank past and present members of the Ferreira Lab for helpful discussions.

## AUTHOR CONTRIBUTIONS

L.M.R.F. and R.W.C. conceived the study. L.M.R.F. supervised the study. L.M.R.F., R.W.C., R.A.R., E.A., S.V., and M.J.R. performed experiments. L.M.R.F., R.W.C., R.A.R., B.G., E.A., A.A.d.C., and S.B. performed data analysis. L.M.R.F. and R.W.C. wrote the manuscript. All authors reviewed and approved the manuscript.

## DECLARATION OF INTERESTS

L.M.R.F. is the inventor on a provisional patent based on results from this work, an inventor on provisional and licensed patents on engineered immune cells, and a consultant with Guidepoint Global and McKesson.

## SUPPLEMENTAL INFORMATION

Supplemental information can be found online at https://doi.org/10.1016/j.omtm.2024.101385.

## REFERENCES

1. Ettenger, R., Chin, H., Kesler, K., Bridges, N., Grimm, P., Reed, E.F., Sarwal, M., Sibley, R., Tsai, E., Warshaw, B., and Kirk, A.D. (2017). Relationship Among Viremia/Viral Infection, Alloimmunity, and Nutritional Parameters in the First Year After Pediatric Kidney Transplantation. Am. J. Transplant. *17*, 1549–1562. https://doi.org/10.1111/ajt.14169.

2. Nelson, J., Alvey, N., Bowman, L., Schulte, J., Segovia, M.C., McDermott, J., Te, H.S., Kapila, N., Levine, D.J., Gottlieb, R.L., et al. (2022). Consensus recommendations for use of maintenance immunosuppression in solid organ transplantation: Endorsed by the American College of Clinical Pharmacy, American Society of Transplantation, and the International Society for Heart and Lung Transplantation. Pharmacotherapy *42*, 599–633. https://doi.org/10.1002/phar.2716.

3. Shivaswamy, V., Boerner, B., and Larsen, J. (2016). Post-Transplant Diabetes Mellitus: Causes, Treatment, and Impact on Outcomes. Endocr. Rev. *37*, 37–61. https://doi.org/10.1210/er.2015-1084.

4. Ghobadinezhad, F., Ebrahimi, N., Mozaffari, F., Moradi, N., Beiranvand, S., Pournazari, M., Rezaei-Tazangi, F., Khorram, R., Afshinpour, M., Robino, R.A., et al. (2022). The emerging role of regulatory cell-based therapy in autoimmune disease. Front. Immunol. *13*, 1075813. https://doi.org/10.3389/fimmu.2022.1075813.

5. Ferreira, L.M.R., Muller, Y.D., Bluestone, J.A., and Tang, Q. (2019). Next-generation regulatory T cell therapy. Nat. Rev. Drug Discov. *18*, 749–769. https://doi.org/10.1038/s41573-019-0041-4.

6. Hori, S., Nomura, T., and Sakaguchi, S. (2003). Control of regulatory T cell development by the transcription factor Foxp3. Science *299*, 1057–1061. https://doi.org/10.1126/science.1079490.

7. Fontenot, J.D., Gavin, M.A., and Rudensky, A.Y. (2003). Foxp3 programs the development and function of CD4+CD25+ regulatory T cells. Nat. Immunol. *4*, 330–336. https://doi.org/10.1038/ni904.

8. Khattri, R., Cox, T., Yasayko, S.A., and Ramsdell, F. (2003). An essential role for Scurfin in CD4+CD25+ T regulatory cells. Nat. Immunol. *4*, 337–342. https://doi.org/10.1038/ni909.

9. Nayer, B., Tan, J.L., Alshoubaki, Y.K., Lu, Y.Z., Legrand, J.M.D., Lau, S., Hu, N., Park, A.J., Wang, X.N., Amann-Zalcenstein, D., et al. (2024). Local administration of regulatory T cells promotes tissue healing. Nat. Commun. *15*, 7863. https://doi.org/10.1038/s41467-024-51353-2.

10. Bluestone, J.A., Buckner, J.H., Fitch, M., Gitelman, S.E., Gupta, S., Hellerstein, M.K., Herold, K.C., Lares, A., Lee, M.R., Li, K., et al. (2015). Type 1 diabetes immunotherapy using polyclonal regulatory T cells. Sci. Transl. Med. *7*, 315ra189. https://doi.org/10.1126/scitranslmed.aad4134.

11. Tang, Q., Leung, J., Peng, Y., Sanchez-Fueyo, A., Lozano, J.J., Lam, A., Lee, K., Greenland, J.R., Hellerstein, M., Fitch, M., et al. (2022). Selective decrease of donor-reactive T(regs) after liver transplantation limits T(reg) therapy for promoting allograft tolerance in humans. Sci. Transl. Med. *14*, eabo2628. https://doi.org/10.1126/scitranslmed.abo2628.

12. Sawitzki, B., Harden, P.N., Reinke, P., Moreau, A., Hutchinson, J.A., Game, D.S., Tang, Q., Guinan, E.C., Battaglia, M., Burlingham, W.J., et al. (2020). Regulatory cell therapy in kidney transplantation (The ONE Study): a harmonised design and analysis of seven non-randomised, single-arm, phase 1/2A trials. Lancet *395*, 1627–1639. https://doi.org/10.1016/S0140-6736(20)30167-7.

13. June, C.H., and Sadelain, M. (2018). Chimeric Antigen Receptor Therapy. N. Engl. J. Med. *379*, 64–73. https://doi.org/10.1056/NEJMra1706169.

14. Cappell, K.M., and Kochenderfer, J.N. (2023). Long-term outcomes following CAR T cell therapy: what we know so far. Nat. Rev. Clin. Oncol. *20*, 359–371. https://doi.org/10.1038/s41571-023-00754-1.

15. Muller, Y.D., Ferreira, L.M.R., Ronin, E., Ho, P., Nguyen, V., Faleo, G., Zhou, Y., Lee, K., Leung, K.K., Skartsis, N., et al. (2021). Precision Engineering of an Anti-HLA-A2 Chimeric Antigen Receptor in Regulatory T Cells for Transplant Immune Tolerance. Front. Immunol. *12*, 686439. https://doi.org/10.3389/fimmu.2021.686439.

16. MacDonald, K.G., Hoeppli, R.E., Huang, Q., Gillies, J., Luciani, D.S., Orban, P.C., Broady, R., and Levings, M.K. (2016). Alloantigen-specific regulatory T cells generated with a chimeric antigen receptor. J. Clin. Invest. *126*, 1413–1424. https://doi.org/10.1172/JCI82771.

17. Noyan, F., Zimmermann, K., Hardtke-Wolenski, M., Knoefel, A., Schulde, E., Geffers, R., Hust, M., Huehn, J., Galla, M., Morgan, M., et al. (2017). Prevention of Allograft Rejection by Use of Regulatory T Cells With an MHC-Specific Chimeric Antigen Receptor. Am. J. Transplant. *17*, 917–930. https://doi.org/10.1111/ajt.14175.

18. Boardman, D.A., Philippeos, C., Fruhwirth, G.O., Ibrahim, M.A.A., Hannen, R.F., Cooper, D., Marelli-Berg, F.M., Watt, F.M., Lechler, R.I., Maher, J., et al. (2017). Expression of a Chimeric Antigen Receptor Specific for Donor HLA Class I Enhances the Potency of Human Regulatory T Cells in Preventing Human Skin Transplant Rejection. Am. J. Transplant. *17*, 931–943. https://doi.org/10.1111/ajt.14185.

19. Bolivar-Wagers, S., Loschi, M.L., Jin, S., Thangavelu, G., Larson, J.H., McDonald-Hyman, C.S., Aguilar, E.G., Saha, A., Koehn, B.H., Hefazi, M., et al. (2022). Murine CAR19 Tregs suppress acute graft-versus-host disease and maintain graft-versus-tumor responses. JCI Insight *7*, e160674. https://doi.org/10.1172/jci.insight.160674.

20. Wagner, J.C., Ronin, E., Ho, P., Peng, Y., and Tang, Q. (2022). Anti-HLA-A2-CAR Tregs prolong vascularized mouse heterotopic heart allograft survival. Am. J. Transplant. *22*, 2237–2245. https://doi.org/10.1111/ajt.17063.

21. Ellis, G.I., Coker, K.E., Winn, D.W., Deng, M.Z., Shukla, D., Bhoj, V., Milone, M.C., Wang, W., Liu, C., Naji, A., et al. (2022). Trafficking and persistence of alloantigen-specific chimeric antigen receptor regulatory T cells in Cynomolgus macaque. Cell Rep. Med. *3*, 100614. https://doi.org/10.1016/j.xcrm.2022.100614.

22. Tenspolde, M., Zimmermann, K., Weber, L.C., Hapke, M., Lieber, M., Dywicki, J., Frenzel, A., Hust, M., Galla, M., Buitrago-Molina, L.E., et al. (2019). Regulatory T cells engineered with a novel insulin-specific chimeric antigen receptor as a candidate immunotherapy for type 1 diabetes. J. Autoimmun. *103*, 102289. https://doi.org/10.1016/j.jaut.2019.05.017.

23. Obarorakpor, N., Patel, D., Boyarov, R., Amarsaikhan, N., Cepeda, J.R., Eastes, D., Robertson, S., Johnson, T., Yang, K., Tang, Q., and Zhang, L. (2023). Regulatory T cells targeting a pathogenic MHC class II: Insulin peptide epitope postpone spontaneous autoimmune diabetes. Front. Immunol. *14*, 1207108. https://doi.org/10.3389/fimmu.2023.1207108.

24. Spanier, J.A., Fung, V., Wardell, C.M., Alkhatib, M.H., Chen, Y., Swanson, L.A., Dwyer, A.J., Weno, M.E., Silva, N., Mitchell, J.S., et al. (2023). Tregs with an MHC class II peptide-specific chimeric antigen receptor prevent autoimmune diabetes in mice. J. Clin. Invest. *133*, e168601. https://doi.org/10.1172/JCI168601.

25. Joffre, O., Santolaria, T., Calise, D., Al Saati, T., Hudrisier, D., Romagnoli, P., and van Meerwijk, J.P.M. (2008). Prevention of acute and chronic allograft rejection with CD4+CD25+Foxp3+ regulatory T lymphocytes. Nat. Med. *14*, 88–92. https://doi.org/10.1038/nm1688.

26. Tang, Q., Henriksen, K.J., Bi, M., Finger, E.B., Szot, G., Ye, J., Masteller, E.L., McDevitt, H., Bonyhadi, M., and Bluestone, J.A. (2004). In vitro-expanded antigen-specific regulatory T cells suppress autoimmune diabetes. J. Exp. Med. *199*, 1455–1465. https://doi.org/10.1084/jem.20040139.

27. Boroughs, A.C., Larson, R.C., Choi, B.D., Bouffard, A.A., Riley, L.S., Schiferle, E., Kulkarni, A.S., Cetrulo, C.L., Ting, D., Blazar, B.R., et al. (2019). Chimeric antigen receptor costimulation domains modulate human regulatory T cell function. JCI Insight *5*, e126194. https://doi.org/10.1172/jci.insight.126194.

28. Wu, X., Chen, P.I., Whitener, R.L., MacDougall, M.S., Coykendall, V.M.N., Yan, H., Kim, Y.B., Harper, W., Pathak, S., Iliopoulou, B.P., et al. (2024). CD39 delineates chimeric antigen receptor regulatory T cell subsets with distinct cytotoxic & regulatory functions against human islets. Front. Immunol. *15*, 1415102. https://doi.org/10.3389/fimmu.2024.1415102.

29. Schreeb, K., Culme-Seymour, E., Ridha, E., Dumont, C., Atkinson, G., Hsu, B., and Reinke, P. (2022). Study Design: Human Leukocyte Antigen Class I Molecule A( *) 02-Chimeric Antigen Receptor Regulatory T Cells in Renal Transplantation. Kidney Int. Rep. *7*, 1258–1267. https://doi.org/10.1016/j.ekir.2022.03.030.

30. Esensten, J.H., Helou, Y.A., Chopra, G., Weiss, A., and Bluestone, J.A. (2016). CD28 Costimulation: From Mechanism to Therapy. Immunity *44*, 973–988. https://doi.org/10.1016/j.immuni.2016.04.020.

31. Holst, J., Wang, H., Eder, K.D., Workman, C.J., Boyd, K.L., Baquet, Z., Singh, H., Forbes, K., Chruscinski, A., Smeyne, R., et al. (2008). Scalable signaling mediated by T cell antigen receptor-CD3 ITAMs ensures effective negative selection and prevents autoimmunity. Nat. Immunol. *9*, 658–666. https://doi.org/10.1038/ni.1611.

32. Li, M.O., and Rudensky, A.Y. (2016). T cell receptor signalling in the control of regulatory T cell differentiation and function. Nat. Rev. Immunol. *16*, 220–233. https://doi.org/10.1038/nri.2016.26.

33. Yan, D., Farache, J., Mingueneau, M., Mathis, D., and Benoist, C. (2015). Imbalanced signal transduction in regulatory T cells expressing the transcription factor FoxP3. Proc. Natl. Acad. Sci. USA *112*, 14942–14947. https://doi.org/10.1073/pnas.1520393112.

34. Crellin, N.K., Garcia, R.V., and Levings, M.K. (2007). Altered activation of AKT is required for the suppressive function of human CD4+CD25+ T regulatory cells. Blood *109*, 2014–2022. https://doi.org/10.1182/blood-2006-07-035279.

35. Bloemberg, D., Nguyen, T., MacLean, S., Zafer, A., Gadoury, C., Gurnani, K., Chattopadhyay, A., Ash, J., Lippens, J., Harcus, D., et al. (2020). A High-Throughput Method for Characterizing Novel Chimeric Antigen Receptors in Jurkat Cells. Mol. Ther. Methods Clin. Dev. *16*, 238–254. https://doi.org/10.1016/j.omtm.2020.01.012.

36. Liu, W., Putnam, A.L., Xu-Yu, Z., Szot, G.L., Lee, M.R., Zhu, S., Gottlieb, P.A., Kapranov, P., Gingeras, T.R., Fazekas de St Groth, B., et al. (2006). CD127 expression inversely correlates with FoxP3 and suppressive function of human CD4+ T reg cells. J. Exp. Med. *203*, 1701–1711. https://doi.org/10.1084/jem.20060772.

37. Seddiki, N., Santner-Nanan, B., Martinson, J., Zaunders, J., Sasson, S., Landay, A., Solomon, M., Selby, W., Alexander, S.I., Nanan, R., et al. (2006). Expression of interleukin (IL)-2 and IL-7 receptors discriminates between human regulatory and activated T cells. J. Exp. Med. *203*, 1693–1700. https://doi.org/10.1084/jem.20060468.

38. Suhoski, M.M., Golovina, T.N., Aqui, N.A., Tai, V.C., Varela-Rohena, A., Milone, M.C., Carroll, R.G., Riley, J.L., and June, C.H. (2007). Engineering artificial antigen-presenting cells to express a diverse array of co-stimulatory molecules. Mol. Ther. *15*, 981–988. https://doi.org/10.1038/mt.sj.6300134.

39. Abbas, A.K., Trotta, E., Simeonov, D.R., Marson, A., and Bluestone, J.A. (2018). Revisiting IL-2: Biology and therapeutic prospects. Sci. Immunol. *3*, eaat1482. https://doi.org/10.1126/sciimmunol.aat1482.

40. Bailey-Bucktrout, S.L., Martinez-Llordella, M., Zhou, X., Anthony, B., Rosenthal, W., Luche, H., Fehling, H.J., and Bluestone, J.A. (2013). Self-antigen-driven activation induces instability of regulatory T cells during an inflammatory autoimmune response. Immunity *39*, 949–962. https://doi.org/10.1016/j.immuni.2013.10.016.

41. Overacre-Delgoffe, A.E., Chikina, M., Dadey, R.E., Yano, H., Brunazzi, E.A., Shayan, G., Horne, W., Moskovitz, J.M., Kolls, J.K., Sander, C., et al. (2017). Interferon-gamma Drives T(reg) Fragility to Promote Anti-tumor Immunity. Cell *169*, 1130–1141.e11. https://doi.org/10.1016/j.cell.2017.05.005.

42. Hoffmann, P., Boeld, T.J., Eder, R., Huehn, J., Floess, S., Wieczorek, G., Olek, S., Dietmaier, W., Andreesen, R., and Edinger, M. (2009). Loss of FOXP3 expression in natural human CD4+CD25+ regulatory T cells upon repetitive in vitro stimulation. Eur. J. Immunol. *39*, 1088–1097. https://doi.org/10.1002/eji.200838904.

43. Nakagawa, H., Sido, J.M., Reyes, E.E., Kiers, V., Cantor, H., and Kim, H.J. (2016). Instability of Helios-deficient Tregs is associated with conversion to a T-effector phenotype and enhanced antitumor immunity. Proc. Natl. Acad. Sci. USA *113*, 6248–6253. https://doi.org/10.1073/pnas.1604765113.

44. Tay, C., Tanaka, A., and Sakaguchi, S. (2023). Tumor-infiltrating regulatory T cells as targets of cancer immunotherapy. Cancer Cell *41*, 450–465. https://doi.org/10.1016/j.ccell.2023.02.014.

45. Zimmerman, C.M., Robino, R.A., Cochrane, R.W., Dominguez, M.D., and Ferreira, L.M.R. (2024). Redirecting Human Conventional and Regulatory T Cells Using Chimeric Antigen Receptors. Methods Mol. Biol. *2748*, 201–241. https://doi.org/10.1007/978-1-0716-3593-3_15.

46. Collison, L.W., and Vignali, D.A.A. (2011). In vitro Treg suppression assays. Methods Mol. Biol. *707*, 21–37. https://doi.org/10.1007/978-1-61737-979-6_2.

47. Dawson, N.A.J., Rosado-Sanchez, I., Novakovsky, G.E., Fung, V.C.W., Huang, Q., McIver, E., Sun, G., Gillies, J., Speck, M., Orban, P.C., et al. (2020). Functional effects of chimeric antigen receptor co-receptor signaling domains in human regulatory T cells. Sci. Transl. Med. *12*, eaaz3866. https://doi.org/10.1126/scitranslmed.aaz3866.

48. Trapani, J.A., and Smyth, M.J. (2002). Functional significance of the perforin/granzyme cell death pathway. Nat. Rev. Immunol. *2*, 735–747. https://doi.org/10.1038/nri911.

49. Boissonnas, A., Scholer-Dahirel, A., Simon-Blancal, V., Pace, L., Valet, F., Kissenpfennig, A., Sparwasser, T., Malissen, B., Fetler, L., and Amigorena, S. (2010). Foxp3+ T cells induce perforin-dependent dendritic cell death in tumor-draining lymph nodes. Immunity *32*, 266–278. https://doi.org/10.1016/j.immuni.2009.11.015.

50. Ludwig-Portugall, I., Hamilton-Williams, E.E., Gottschalk, C., and Kurts, C. (2008). Cutting edge: CD25+ regulatory T cells prevent expansion and induce apoptosis of B cells specific for tissue autoantigens. J. Immunol. *181*, 4447–4451. https://doi.org/10.4049/jimmunol.181.7.4447.

51. Cao, X., Cai, S.F., Fehniger, T.A., Song, J., Collins, L.I., Piwnica-Worms, D.R., and Ley, T.J. (2007). Granzyme B and perforin are important for regulatory T cell-mediated suppression of tumor clearance. Immunity *27*, 635–646. https://doi.org/10.1016/j.immuni.2007.08.014.

52. Grossman, W.J., Verbsky, J.W., Barchet, W., Colonna, M., Atkinson, J.P., and Ley, T.J. (2004). Human T regulatory cells can use the perforin pathway to cause autologous target cell death. Immunity *21*, 589–601. https://doi.org/10.1016/j.immuni.2004.09.002.

53. Brinkman, E.K., Chen, T., Amendola, M., and van Steensel, B. (2014). Easy quantitative assessment of genome editing by sequence trace decomposition. Nucleic Acids Res. *42*, e168. https://doi.org/10.1093/nar/gku936.

54. Jennings, E., Elliot, T.A.E., Thawait, N., Kanabar, S., Yam-Puc, J.C., Ono, M., Toellner, K.M., Wraith, D.C., Anderson, G., and Bending, D. (2020). Nr4a1 and Nr4a3 Reporter Mice Are Differentially Sensitive to T Cell Receptor Signal Strength and Duration. Cell Rep. *33*, 108328. https://doi.org/10.1016/j.celrep.2020.108328.

55. Sundstedt, A., O'Neill, E.J., Nicolson, K.S., and Wraith, D.C. (2003). Role for IL-10 in suppression mediated by peptide-induced regulatory T cells in vivo. J. Immunol. *170*, 1240–1248. https://doi.org/10.4049/jimmunol.170.3.1240.

56. Collison, L.W., Workman, C.J., Kuo, T.T., Boyd, K., Wang, Y., Vignali, K.M., Cross, R., Sehy, D., Blumberg, R.S., and Vignali, D.A.A. (2007). The inhibitory cytokine IL-35 contributes to regulatory T-cell function. Nature *450*, 566–569. https://doi.org/10.1038/nature06306.

57. Kidani, Y., Nogami, W., Yasumizu, Y., Kawashima, A., Tanaka, A., Sonoda, Y., Tona, Y., Nashiki, K., Matsumoto, R., Hagiwara, M., et al. (2022). CCR8-targeted specific depletion of clonally expanded Treg cells in tumor tissues evokes potent tumor immunity with long-lasting memory. Proc. Natl. Acad. Sci. USA *119*, e2114282119. https://doi.org/10.1073/pnas.2114282119.

58. Mercer, F., Kozhaya, L., and Unutmaz, D. (2010). Expression and function of TNF and IL-1 receptors on human regulatory T cells. PLoS One *5*, e8639. https://doi.org/10.1371/journal.pone.0008639.

59. Subramanian, A., Tamayo, P., Mootha, V.K., Mukherjee, S., Ebert, B.L., Gillette, M.A., Paulovich, A., Pomeroy, S.L., Golub, T.R., Lander, E.S., and Mesirov, J.P. (2005). Gene set enrichment analysis: a knowledge-based approach for interpreting genome-wide expression profiles. Proc. Natl. Acad. Sci. USA *102*, 15545–15550. https://doi.org/10.1073/pnas.0506580102.

60. Thornton, A.M., and Shevach, E.M. (2000). Suppressor effector function of CD4+CD25+ immunoregulatory T cells is antigen nonspecific. J. Immunol. *164*, 183–190. https://doi.org/10.4049/jimmunol.164.1.183.

61. Elgueta, R., Benson, M.J., de Vries, V.C., Wasiuk, A., Guo, Y., and Noelle, R.J. (2009). Molecular mechanism and function of CD40/CD40L engagement in the immune system. Immunol. Rev. *229*, 152–172. https://doi.org/10.1111/j.1600-065X.2009.00782.x.

62. Gu, J., Ni, X., Pan, X., Lu, H., Lu, Y., Zhao, J., Guo Zheng, S., Hippen, K.L., Wang, X., and Lu, L. (2017). Human CD39(hi) regulatory T cells present stronger stability and function under inflammatory conditions. Cell. Mol. Immunol. *14*, 521–528. https://doi.org/10.1038/cmi.2016.30.

63. Harshe, R.P., Xie, A., Vuerich, M., Frank, L.A., Gromova, B., Zhang, H., Robles, R.J., Mukherjee, S., Csizmadia, E., Kokkotou, E., et al. (2020). Endogenous antisense RNA curbs CD39 expression in Crohn's disease. Nat. Commun. *11*, 5894. https://doi.org/10.1038/s41467-020-19692-y.

64. Bin Dhuban, K., d'Hennezel, E., Nashi, E., Bar-Or, A., Rieder, S., Shevach, E.M., Nagata, S., and Piccirillo, C.A. (2015). Coexpression of TIGIT and FCRL3 identifies Helios+ human memory regulatory T cells. J. Immunol. *194*, 3687–3696. https://doi.org/10.4049/jimmunol.1401803.

65. Joller, N., Lozano, E., Burkett, P.R., Patel, B., Xiao, S., Zhu, C., Xia, J., Tan, T.G., Sefik, E., Yajnik, V., et al. (2014). Treg cells expressing the coinhibitory molecule TIGIT selectively inhibit proinflammatory Th1 and Th17 cell responses. Immunity *40*, 569–581. https://doi.org/10.1016/j.immuni.2014.02.012.

66. Lee, D.J. (2020). The relationship between TIGIT(+) regulatory T cells and autoimmune disease. Int. Immunopharmacol. *83*, 106378. https://doi.org/10.1016/j.intimp.2020.106378.

67. Hu, X., and Ivashkiv, L.B. (2009). Cross-regulation of signaling pathways by interferon-gamma: implications for immune responses and autoimmune diseases. Immunity *31*, 539–550. https://doi.org/10.1016/j.immuni.2009.09.002.

68. DuPage, M., and Bluestone, J.A. (2016). Harnessing the plasticity of CD4(+) T cells to treat immune-mediated disease. Nat. Rev. Immunol. *16*, 149–163. https://doi.org/10.1038/nri.2015.18.

69. Imura, Y., Ando, M., Kondo, T., Ito, M., and Yoshimura, A. (2020). CD19-targeted CAR regulatory T cells suppress B cell pathology without GvHD. JCI Insight *5*, e136185. https://doi.org/10.1172/jci.insight.136185.

70. Hoffmann, P., Eder, R., Boeld, T.J., Doser, K., Piseshka, B., Andreesen, R., and Edinger, M. (2006). Only the CD45RA+ subpopulation of CD4+CD25high T cells gives rise to homogeneous regulatory T-cell lines upon in vitro expansion. Blood *108*, 4260–4267. https://doi.org/10.1182/blood-2006-06-027409.

71. Arroyo Hornero, R., Betts, G.J., Sawitzki, B., Vogt, K., Harden, P.N., and Wood, K.J. (2017). CD45RA Distinguishes CD4+CD25+CD127-/low TSDR Demethylated Regulatory T Cell Subpopulations With Differential Stability and Susceptibility to Tacrolimus-Mediated Inhibition of Suppression. Transplantation *101*, 302–309. https://doi.org/10.1097/TP.0000000000001278.

72. Doglio, M., Ugolini, A., Bercher-Brayer, C., Camisa, B., Toma, C., Norata, R., Del Rosso, S., Greco, R., Ciceri, F., Sanvito, F., et al. (2024). Regulatory T cells expressing CD19-targeted chimeric antigen receptor restore homeostasis in Systemic Lupus

Erythematosus. Nat. Commun. *15*, 2542. https://doi.org/10.1038/s41467-024-46448-9.

73. Lei, H., Kuchenbecker, L., Streitz, M., Sawitzki, B., Vogt, K., Landwehr-Kenzel, S., Millward, J., Juelke, K., Babel, N., Neumann, A., et al. (2015). Human CD45RA(-) FoxP3(hi) Memory-Type Regulatory T Cells Show Distinct TCR Repertoires With Conventional T Cells and Play an Important Role in Controlling Early Immune Activation. Am. J. Transplant. *15*, 2625–2635. https://doi.org/10.1111/ajt.13315.

74. Schmid, D.A., Irving, M.B., Posevitz, V., Hebeisen, M., Posevitz-Fejfar, A., Sarria, J.C.F., Gomez-Eerland, R., Thome, M., Schumacher, T.N.M., Romero, P., et al. (2010). Evidence for a TCR affinity threshold delimiting maximal CD8 T cell function. J. Immunol. *184*, 4936–4946. https://doi.org/10.4049/jimmunol.1000173.

75. Chen, L., and Flies, D.B. (2013). Molecular mechanisms of T cell co-stimulation and co-inhibition. Nat. Rev. Immunol. *13*, 227–242. https://doi.org/10.1038/nri3405.

76. Ghorashian, S., Kramer, A.M., Onuoha, S., Wright, G., Bartram, J., Richardson, R., Albon, S.J., Casanovas-Company, J., Castro, F., Popova, B., et al. (2019). Enhanced CAR T cell expansion and prolonged persistence in pediatric patients with ALL treated with a low-affinity CD19 CAR. Nat. Med. *25*, 1408–1414. https://doi.org/10.1038/s41591-019-0549-5.

77. Salter, A.I., Ivey, R.G., Kennedy, J.J., Voillet, V., Rajan, A., Alderman, E.J., Voytovich, U.J., Lin, C., Sommermeyer, D., Liu, L., et al. (2018). Phosphoproteomic analysis of chimeric antigen receptor signaling reveals kinetic and quantitative differences that affect cell function. Sci. Signal. *11*, eaat6753. https://doi.org/10.1126/scisignal.aat6753.

78. Fisher, J.D., Zhang, W., Balmert, S.C., Aral, A.M., Acharya, A.P., Kulahci, Y., Li, J., Turnquist, H.R., Thomson, A.W., Solari, M.G., et al. (2020). In situ recruitment of regulatory T cells promotes donor-specific tolerance in vascularized composite allotransplantation. Sci. Adv. *6*, eaax8429. https://doi.org/10.1126/sciadv.aax8429.

79. Pandiyan, P., Zheng, L., Ishihara, S., Reed, J., and Lenardo, M.J. (2007). CD4+CD25+Foxp3+ regulatory T cells induce cytokine deprivation-mediated apoptosis of effector CD4+ T cells. Nat. Immunol. *8*, 1353–1362. https://doi.org/10.1038/ni1536.

80. Dalton, D.K., Pitts-Meek, S., Keshav, S., Figari, I.S., Bradley, A., and Stewart, T.A. (1993). Multiple defects of immune cell function in mice with disrupted interferon-gamma genes. Science *259*, 1739–1742. https://doi.org/10.1126/science.8456300.

81. Marson, A., Kretschmer, K., Frampton, G.M., Jacobsen, E.S., Polansky, J.K., MacIsaac, K.D., Levine, S.S., Fraenkel, E., von Boehmer, H., and Young, R.A. (2007). Foxp3 occupancy and regulation of key target genes during T-cell stimulation. Nature *445*, 931–935. https://doi.org/10.1038/nature05478.

82. Esposito, M., Ruffini, F., Bergami, A., Garzetti, L., Borsellino, G., Battistini, L., Martino, G., and Furlan, R. (2010). IL-17- and IFN-gamma-secreting Foxp3+ T cells infiltrate the target tissue in experimental autoimmunity. J. Immunol. *185*, 7467–7473. https://doi.org/10.4049/jimmunol.1001519.

83. Duhen, T., Duhen, R., Lanzavecchia, A., Sallusto, F., and Campbell, D.J. (2012). Functionally distinct subsets of human FOXP3+ Treg cells that phenotypically mirror effector Th cells. Blood *119*, 4430–4440. https://doi.org/10.1182/blood-2011-11-392324.

84. Schoenbrunn, A., Frentsch, M., Kohler, S., Keye, J., Dooms, H., Moewes, B., Dong, J., Loddenkemper, C., Sieper, J., Wu, P., et al. (2012). A converse 4-1BB and CD40 ligand expression pattern delineates activated regulatory T cells (Treg) and conventional T cells enabling direct isolation of alloantigen-reactive natural Foxp3+ Treg. J. Immunol. *189*, 5985–5994. https://doi.org/10.4049/jimmunol.1201090.

85. Nowak, A., Lock, D., Bacher, P., Hohnstein, T., Vogt, K., Gottfreund, J., Giehr, P., Polansky, J.K., Sawitzki, B., Kaiser, A., et al. (2018). CD137+CD154- Expression As a Regulatory T Cell (Treg)-Specific Activation Signature for Identification and Sorting of Stable Human Tregs from In Vitro Expansion Cultures. Front. Immunol. *9*, 199. https://doi.org/10.3389/fimmu.2018.00199.

86. Shen, X., Wang, Y., Gao, F., Ren, F., Busuttil, R.W., Kupiec-Weglinski, J.W., and Zhai, Y. (2009). CD4 T cells promote tissue inflammation via CD40 signaling without de novo activation in a murine model of liver ischemia/reperfusion injury. Hepatology *50*, 1537–1546. https://doi.org/10.1002/hep.23153.

87. Zhang, N., Schröppel, B., Lal, G., Jakubzick, C., Mao, X., Chen, D., Yin, N., Jessberger, R., Ochando, J.C., Ding, Y., and Bromberg, J.S. (2009). Regulatory T cells sequentially migrate from inflamed tissues to draining lymph nodes to suppress the alloimmune response. Immunity *30*, 458–469. https://doi.org/10.1016/j.immuni.2008.12.022.

88. Mao, R., Kong, W., and He, Y. (2022). The affinity of antigen-binding domain on the antitumor efficacy of CAR T cells: Moderate is better. Front. Immunol. *13*, 1032403. https://doi.org/10.3389/fimmu.2022.1032403.

89. Hogquist, K.A., and Jameson, S.C. (2014). The self-obsession of T cells: how TCR signaling thresholds affect fate 'decisions' and effector function. Nat. Immunol. *15*, 815–823. https://doi.org/10.1038/ni.2938.

90. Stone, J.D., Chervin, A.S., and Kranz, D.M. (2009). T-cell receptor binding affinities and kinetics: impact on T-cell activity and specificity. Immunology *126*, 165–176. https://doi.org/10.1111/j.1365-2567.2008.03015.x.

91. Majzner, R.G., Rietberg, S.P., Sotillo, E., Dong, R., Vachharajani, V.T., Labanieh, L., Myklebust, J.H., Kadapakkam, M., Weber, E.W., Tousley, A.M., et al. (2020). Tuning the Antigen Density Requirement for CAR T-cell Activity. Cancer Discov. *10*, 702–723. https://doi.org/10.1158/2159-8290.CD-19-0945.

92. Muller, Y.D., Nguyen, D.P., Ferreira, L.M.R., Ho, P., Raffin, C., Valencia, R.V.B., Congrave-Wilson, Z., Roth, T.L., Eyquem, J., Van Gool, F., et al. (2021). The CD28-Transmembrane Domain Mediates Chimeric Antigen Receptor Heterodimerization With CD28. Front. Immunol. *12*, 639818. https://doi.org/10.3389/fimmu.2021.639818.

93. Ferreira, L., Kaul, A., Guerrero-Moreno, R., Fontenot, J.D., Bluestone, J.A., and Tang, Q. (2018). Tailoring a new generation of chimeric antigen receptors for regulatory T cells. J. Immunol. *200*, 176.

94. Uenishi, G.I., Repic, M., Yam, J.Y., Landuyt, A., Saikumar-Lakshmi, P., Guo, T., Zarin, P., Sassone-Corsi, M., Chicoine, A., Kellogg, H., et al. (2024). GNTI-122: an autologous antigen-specific engineered Treg cell therapy for type 1 diabetes. JCI Insight *9*, e171844. https://doi.org/10.1172/jci.insight.171844.

95. Fung, V.C.W., Rosado-Sánchez, I., and Levings, M.K. (2021). Transduction of Human T Cell Subsets with Lentivirus. Methods Mol. Biol. *2285*, 227–254. https://doi.org/10.1007/978-1-0716-1311-5_19.

96. Dobin, A., Davis, C.A., Schlesinger, F., Drenkow, J., Zaleski, C., Jha, S., Batut, P., Chaisson, M., and Gingeras, T.R. (2013). STAR: ultrafast universal RNA-seq aligner. Bioinformatics *29*, 15–21. https://doi.org/10.1093/bioinformatics/bts635.

97. Liao, Y., Smyth, G.K., and Shi, W. (2014). featureCounts: an efficient general purpose program for assigning sequence reads to genomic features. Bioinformatics *30*, 923–930. https://doi.org/10.1093/bioinformatics/btt656.

98. Love, M.I., Huber, W., and Anders, S. (2014). Moderated estimation of fold change and dispersion for RNA-seq data with DESeq2. Genome Biol. *15*, 550. https://doi.org/10.1186/s13059-014-0550-8.

99. Ge, S.X., Son, E.W., and Yao, R. (2018). iDEP: an integrated web application for differential expression and pathway analysis of RNA-Seq data. BMC Bioinf. *19*, 534. https://doi.org/10.1186/s12859-018-2486-6.

**OMTM, Volume *32***

## Supplemental information

# High-affinity chimeric antigen receptor signaling induces an inflammatory program in human regulatory T cells

**Russell W. Cochrane, Rob A. Robino, Bryan Granger, Eva Allen, Silvia Vaena, Martin J. Romeo, Aguirre A. de Cubas, Stefano Berto, and Leonardo M.R. Ferreira**

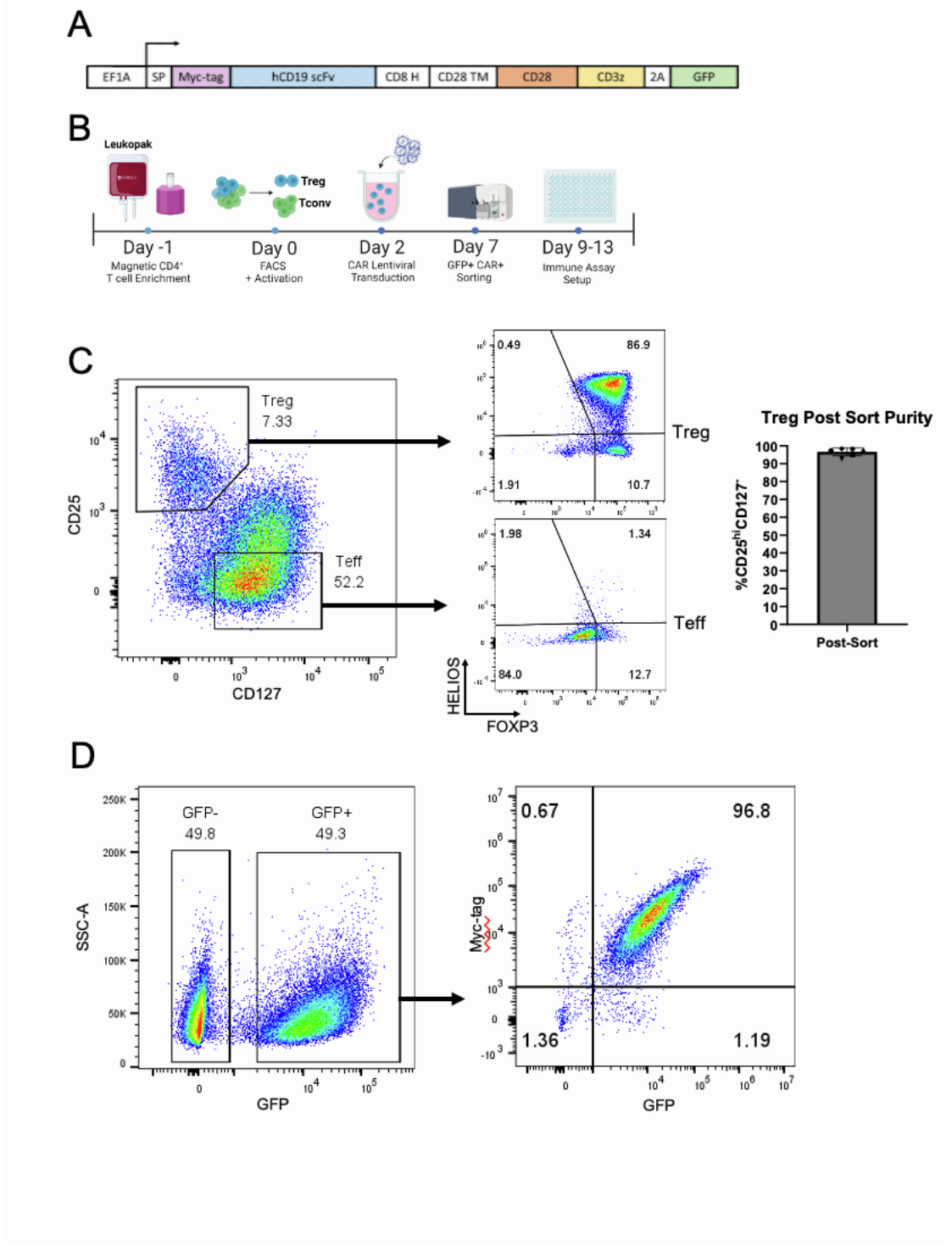
A
EF1A
SP
Myc-tag
hCD19 scFv
CD8 H
CD28 TM
CD28
CD3z
2A
GFP
B
Leukopak
Treg
Tconv
Day -1
Magnetic CD4+
T cell Enrichment
Day 0
FACS
+ Activation
Day 2
CAR Lentiviral
Transduction
Day 7
GFP+ CAR+
Sorting
Day 9-13
Immune Assay
Setup
C
Treg
7.33
Teff
52.2
CD25
CD127
0.49
86.9
1.91
10.7
Treg
1.98
1.34
Teff
84.0
12.7
HELIOS
FOXP3
Treg Post Sort Purity
%CD25hiCD127-
Post-Sort
D
GFP-
49.8
GFP+
49.3
SSC-A
GFP
0.67
96.8
1.36
1.19
Myc-tag
GFP

**Figure S1. Human CAR Treg generation.** (A) Chimeric antigen receptor (CAR) construct used in this study. (B) Workflow to isolate human CD4+ regulatory T cells (Tregs) and effector T cells (Teff), introduce a CAR, expand, and sort CAR-expressing cells for immune assays. (C) Representative dot plots of Treg sorting strategy with $CD25^{hi}CD127^{low}$ Tregs and $CD25^{low}CD127^{hi}$ Teff on the left and Treg post sort phenotype assessment with $FOXP3^{+}HELIOS^{+}$ Tregs and $FOXP3^{-}HELIOS^{-}$ Teff cells on the right. Post-sort purity of $CD25^{hi}CD127^{low}$ Tregs across multiple donors (n=6). (D) Representative dot plots of Treg transduction efficiency with CD19CAR-2A-GFP lentivirus, based on GFP expression on the left and CAR surface expression (Myc-tag) and reporter gene expression (GFP) after sorting GFP+ cells on the right.

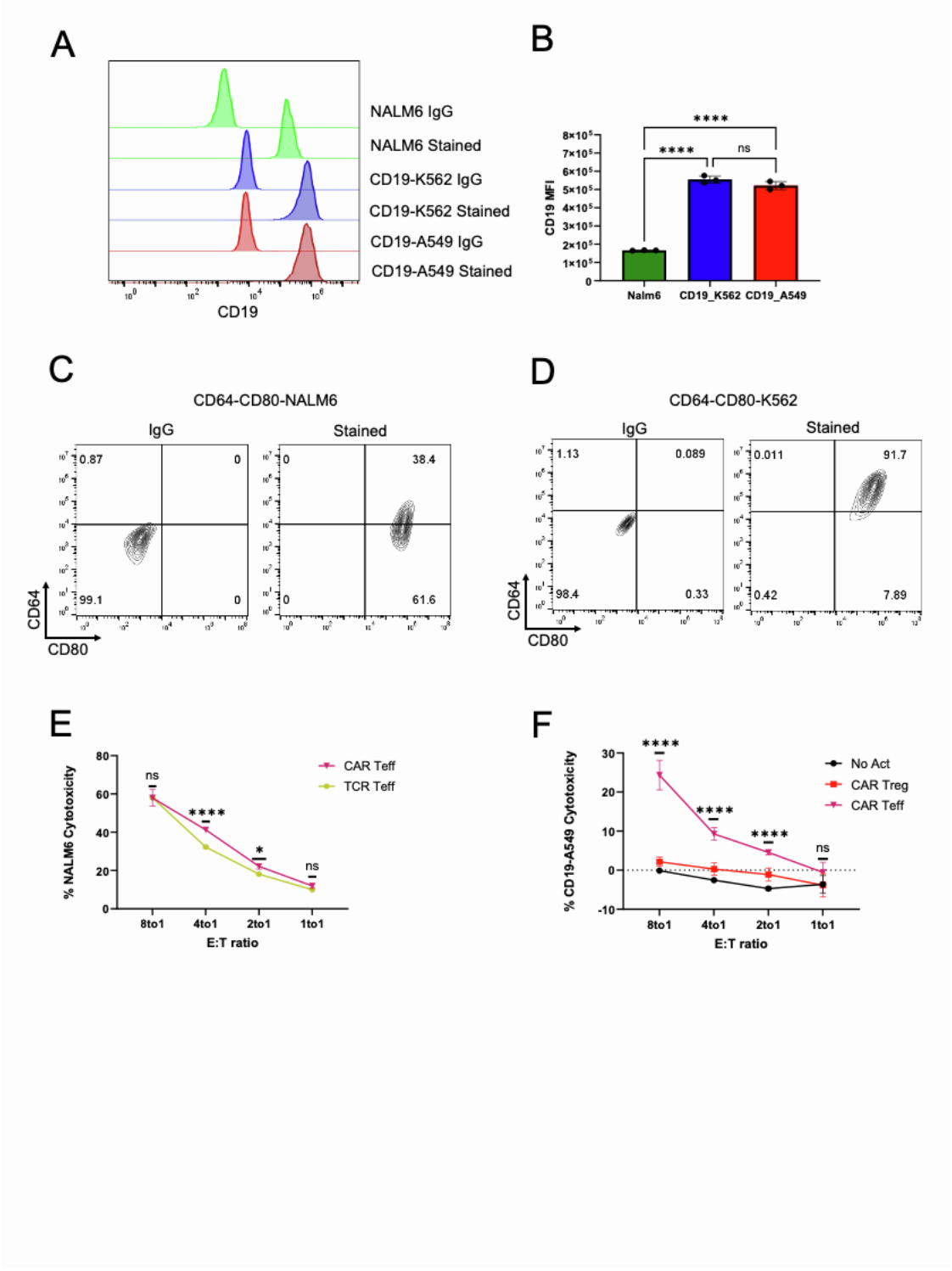
A
NALM6 IgG
NALM6 Stained
CD19-K562 IgG
CD19-K562 Stained
CD19-A549 IgG
CD19-A549 Stained
CD19
B
CD19 MFI
****
****
ns
Nalm6
CD19_K562
CD19_A549
C
CD64-CD80-NALM6
IgG
Stained
0.87
0
99.1
0
0
38.4
0
61.6
CD64
CD80
D
CD64-CD80-K562
IgG
Stained
1.13
0.089
98.4
0.33
0.011
91.7
0.42
7.89
CD64
CD80
E
% NALM6 Cytotoxicity
CAR Teff
TCR Teff
ns
****
*
ns
8to1
4to1
2to1
1to1
E:T ratio
F
% CD19-A549 Cytotoxicity
No Act
CAR Treg
CAR Teff
****
****
****
ns
8to1
4to1
2to1
1to1
E:T ratio

**Figure S2. Characterization of target cell lines and cytotoxicity towards them.** (A) Histograms of CD19 surface expression on CD19-K562, NALM6, and CD19-A549 target cells. (B) Mean fluorescence intensity (MFI) of CD19 surface expression on CD19-K562, NALM6, and CD19-A549 target cells. (C) Contour plot of CD80 and CD64 surface expression on CD64-CD80-NALM6 cells. (D) Contour plot of CD80 and CD64 surface expression on CD64-CD80-K562 cells. (E) Effector T (Teff) cell cytotoxicity towards NALM6 cells at different effector to target (E:T) ratios. (F) Treg and Teff cytotoxicity towards CD19-A549 cells at different E:T ratios. Values represent technical replicates of representative experiment. Bars represent mean ± standard deviation (SD). To determine statistical significance, one way ANOVA with Tukey's multiple comparison correction was used in Figure S2B, and two-way ANOVA test with Tukey's multiple comparison correction was used in Figure S2E and S2F. ****, $p < 0.0001$; ***, $p < 0.001$; **, $p < 0.01$; *, $p < 0.05$; ns, not significant.

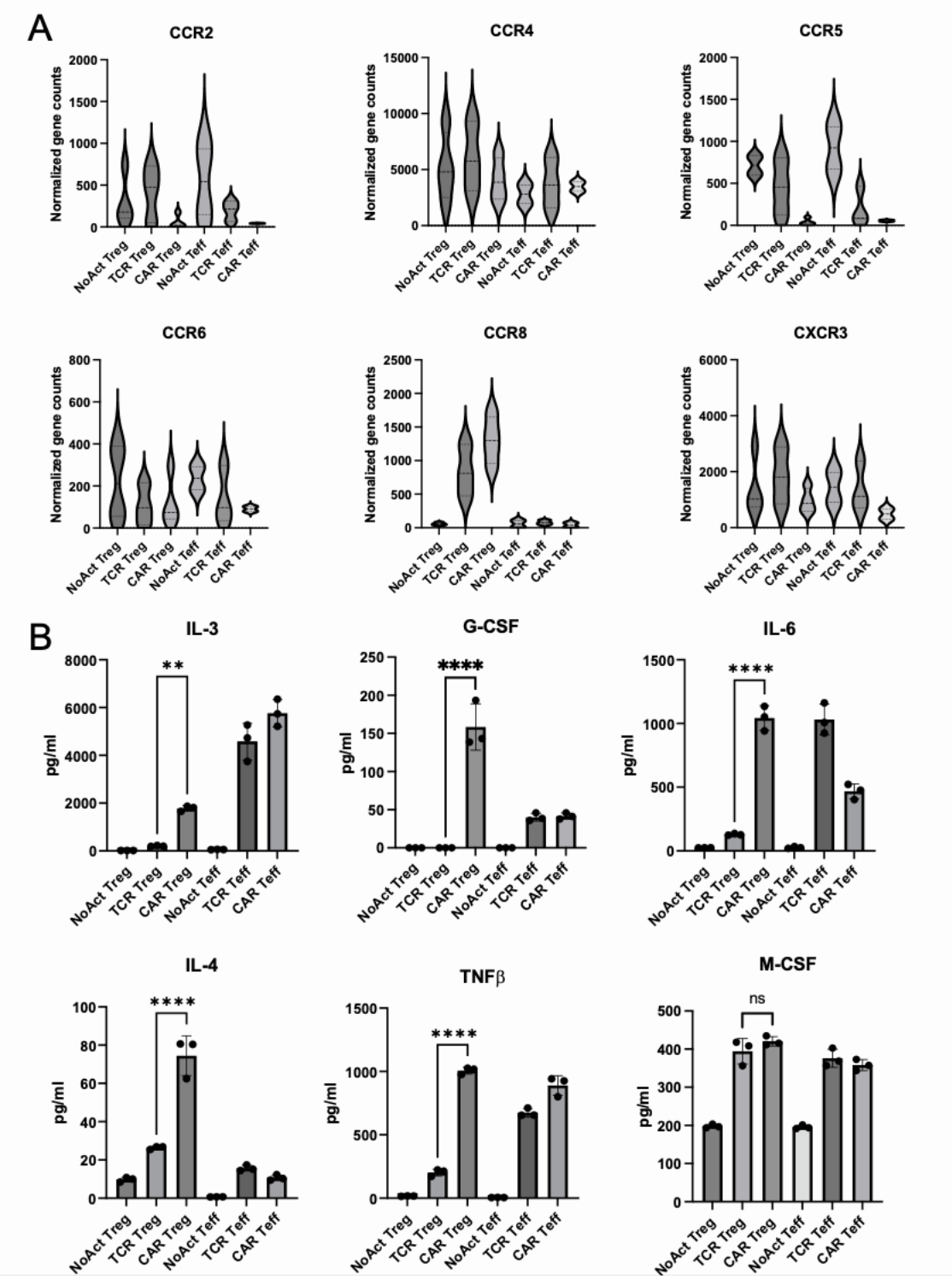
A
CCR2
CCR4
CCR5
CCR6
CCR8
CXCR3
Normalized gene counts
NoAct Treg
TCR Treg
CAR Treg
NoAct Teff
TCR Teff
CAR Teff
B
IL-3
G-CSF
IL-6
IL-4
TNFβ
M-CSF
pg/ml
**
****
ns

**Figure S3. Chemokine and Cytokine Expression of Tregs and Teff cells.** (A) Chemokine receptor gene expression levels in No Act Tregs, TCR Tregs, CAR Tregs, No Act Teff, TCR Teff, and CAR Teff 24 hours post activation. Violins represent mean ± standard deviation (SD) of RNA-seq gene counts across blood donors. (B) Cytokine secretion levels by No Act Tregs, TCR Tregs, CAR Tregs, No Act Teff, TCR Teff, and CAR Teff 48 hours post activation. Values represent technical replicates of representative experiment. Bars represent mean ± SD. One-way ANOVA test with Tukey's multiple comparison correction was used to assess statistical significance. ****, $p < 0.0001$; ***, $p < 0.001$; **, $p < 0.01$; *, $p < 0.05$; ns, not significant.

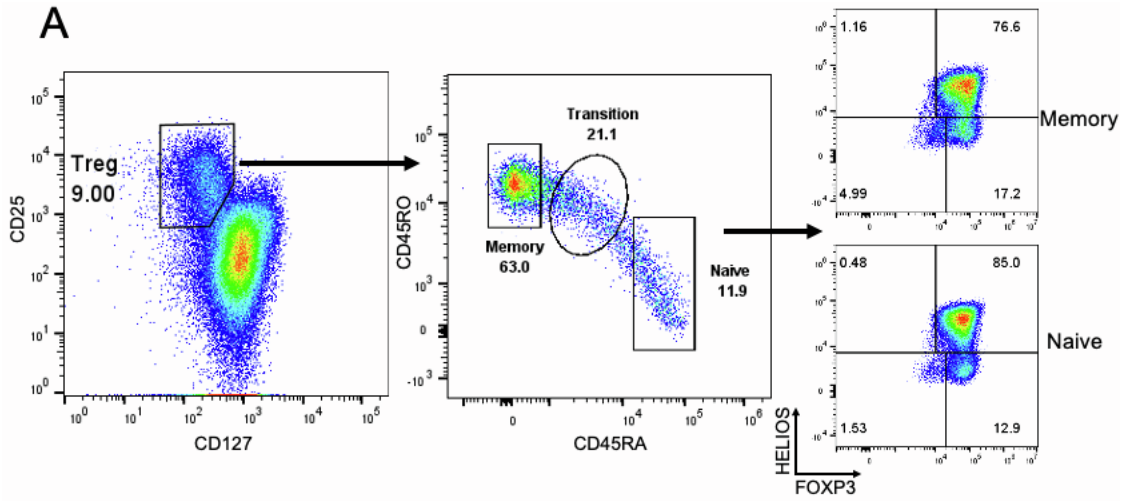
A
Treg
9.00
CD25
CD127
Transition
21.1
Memory
63.0
Naive
11.9
CD45RO
CD45RA
1.16
76.6
Memory
4.99
17.2
0.48
85.0
Naive
1.53
12.9
HELIOS
FOXP3

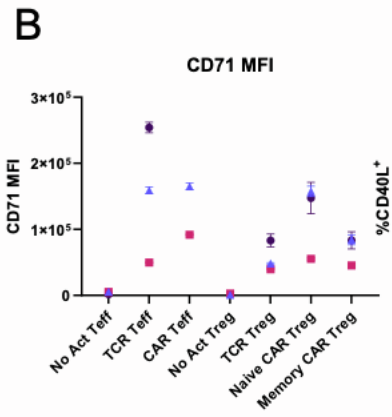
B
CD71 MFI
CD71 MFI
No Act Teff
TCR Teff
CAR Teff
No Act Treg
TCR Treg
Naive CAR Treg
Memory CAR Treg

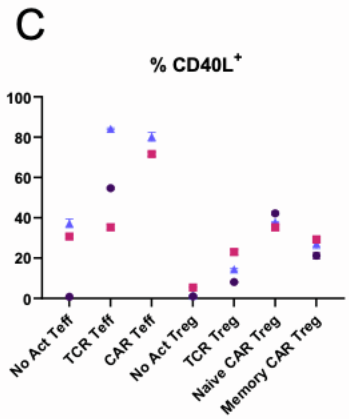
C
% CD40L+
%CD40L+
No Act Teff
TCR Teff
CAR Teff
No Act Treg
TCR Treg
Naive CAR Treg
Memory CAR Treg

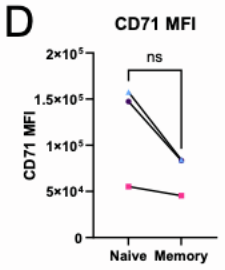
D
CD71 MFI
ns
CD71 MFI
Naive
Memory

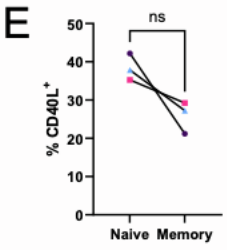
E
ns
% CD40L+
Naive
Memory

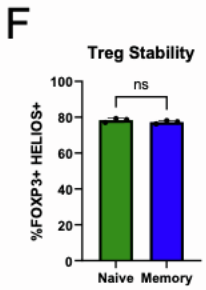
F
Treg Stability
ns
%FOXP3+ HELIOS+
Naive
Memory

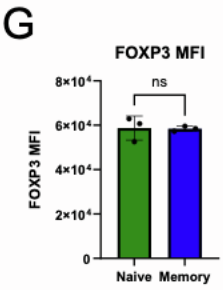
G
FOXP3 MFI
ns
FOXP3 MFI
Naive
Memory

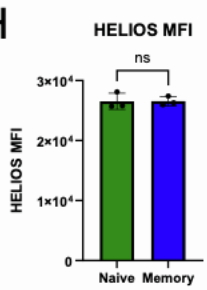
H
HELIOS MFI
ns
HELIOS MFI
Naive
Memory

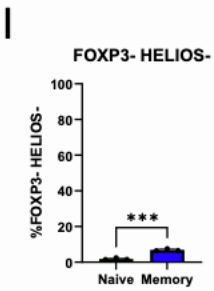
I
FOXP3- HELIOS-
***
%FOXP3- HELIOS-
Naive
Memory

**Figure S4. CAR activation in naïve or memory Tregs results in phenotypically similar Tregs.** (A) Representative dot plots of sorting strategy to obtain $CD25^{hi}CD127^{low}$ Tregs of either $CD45RO^{+}CD45RA^{-}$ (memory), $CD45RO^{+}CD45RA^{+}$ (transition), and $CD45RO^{+}CD45RA^{-}$ (naïve) phenotype on the left. Naïve and memory Treg post sort phenotype (FOXP3 and HELIOS expression) assessment on the right. (B) Summary data across donors (n=3) of CD71 surface expression 48h after Treg and effector T (Teff) cell activation. (C) Summary data across donors (n=3) of CD40L surface expression 48h after Treg and Teff cell activation. (D) CD71 surface expression (mean fluorescence intensity – MFI) 48h after CAR naïve and memory Treg activation. (E) CD40L surface expression ($\%CD40L^{+}$ cells) 48h after CAR naïve and memory Treg activation. (F) Percentage of $FOXP3^{+}HELIOS^{+}$ cells in CAR naïve and memory Tregs eight days post CAR activation.(G) FOXP3 MFI in CAR naïve and memory Tregs eight days post CAR activation (H) HELIOS MFI in CAR naïve and memory Tregs eight days post CAR activation. (I) Percentage of $FOXP3^{-}HELIOS^{-}$ cells in CAR naïve and memory Tregs eight days post CAR activation. For Figure S4B and S4C, values represent mean ± standard deviation (SD) of technical triplicates per blood donor (n=3). For Figure S4D and S4E, values represent mean of technical triplicates per blood donor (n=3), with lines collecting the data points from the same donor. Statistical significance was assessed using paired Student's t test. For Figure S4F, S4G, S4H, and S4I, values represent technical replicates of representative experiment. Bars represent mean ± SD. Statistical significance was assessed using unpaired Student's t test. ****, $p < 0.0001$; ***, $p < 0.001$; **, $p < 0.01$; *, $p < 0.05$; ns, not significant.

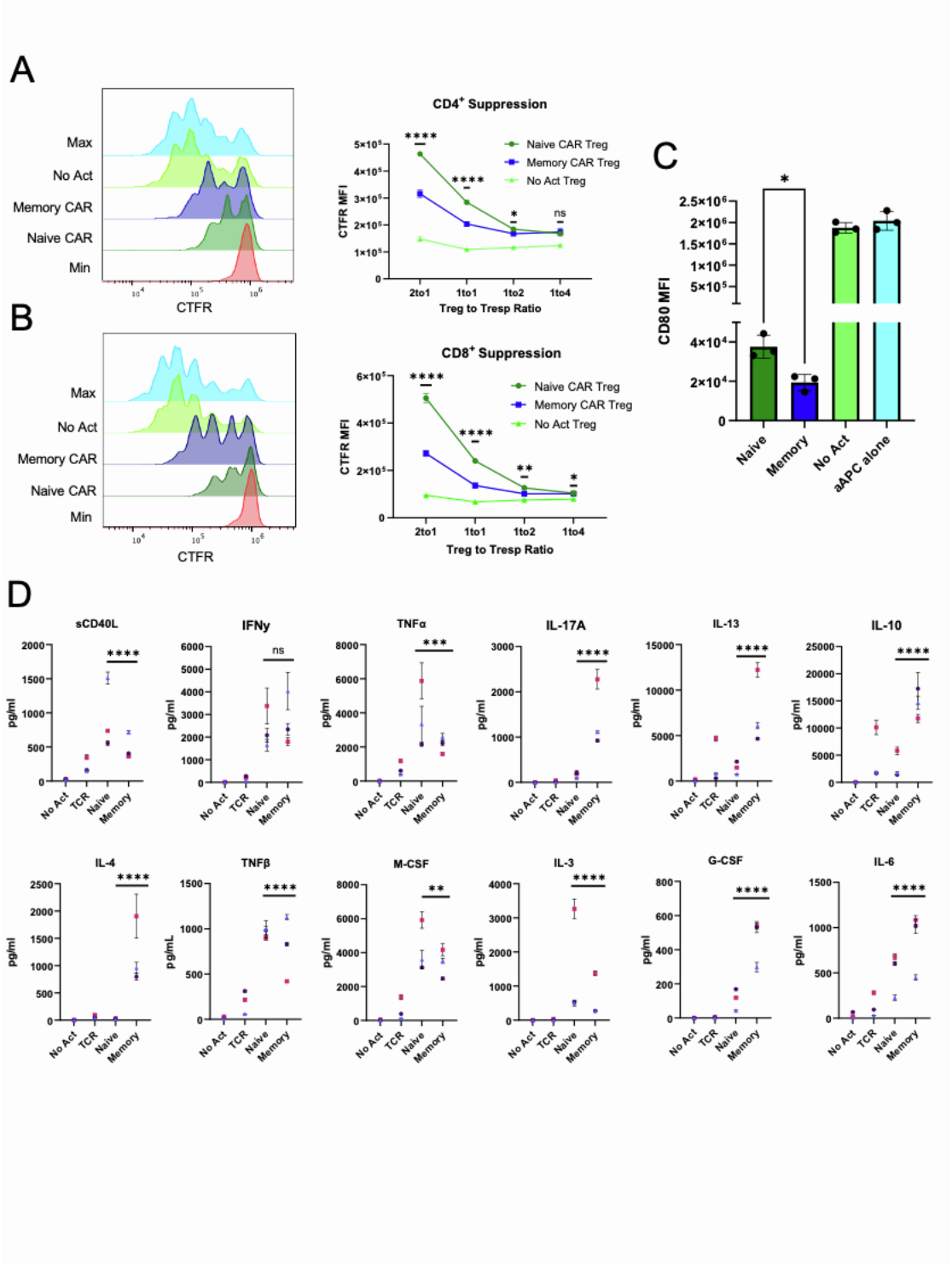
A
Max
No Act
Memory CAR
Naive CAR
Min
CTFR
CD4+ Suppression
Naive CAR Treg
Memory CAR Treg
No Act Treg
CTFR MFI
Treg to Tresp Ratio
2to1
1to1
1to2
1to4
B
CD8+ Suppression
C
CD80 MFI
Naive
Memory
No Act
aAPC alone
D
sCD40L
IFNγ
TNFα
IL-17A
IL-13
IL-10
IL-4
TNFβ
M-CSF
IL-3
G-CSF
IL-6
pg/ml
No Act
TCR
Naive
Memory

**Figure S5. CAR activation leads to the same levels of IFNγ secretion in naïve and memory Tregs.** (A) On the left, representative flow cytometry histograms of proliferation of Cell Trace Far Red (CTFR)-labeled $CD4^+$ T responder (Tresp) cells co-cultured with activated CAR Tregs at a 2: 1 Treg to Tresp ratio. On the right, suppression of proliferation of CTFR-labeled $CD4^+$ Tresp cells by Tregs at various Treg to Tresp ratios (2:1, 1:1, 1:2, and 1:4). (B) On the left, representative flow cytometry histogram of proliferation of CTFR-labeled $CD8^+$ Tresp cells co-cultured with activated CAR Tregs at a 2:1 Treg to Tresp ratio. On the right, suppression of proliferation of CTFR-labeled $CD8^+$ Tresp cells by Tregs at various Treg to Tresp ratios (2:1, 1:1, 1:2, and 1:4). Values represent mean ± standard deviation (SD) of technical replicates of representative experiment, with statistical significance computed by one-way ANOVA with Tukey's multiple comparison correction. (C) Representative histograms of downregulation of CD80 surface expression in CD80-CD64-NALM6 cells (aAPC – artificial antigen presenting cells) by Tregs. Bars represent mean ± SD of technical replicates of representative experiment, with statistical significance assessed by unpaired Student's t test. (D) Levels of cytokines secreted by No Act Tregs, TCR Tregs, CAR naïve Tregs, and CAR memory Tregs 48h post-activation. Values represent mean ± SD of technical triplicates per blood donor (n=3), with statistical significance assessed by one-way ANOVA test with Tukey's multiple comparison correction. ****, $p < 0.0001$; ***, $p < 0.001$; **, $p < 0.01$; *, $p < 0.05$; ns, not significant.

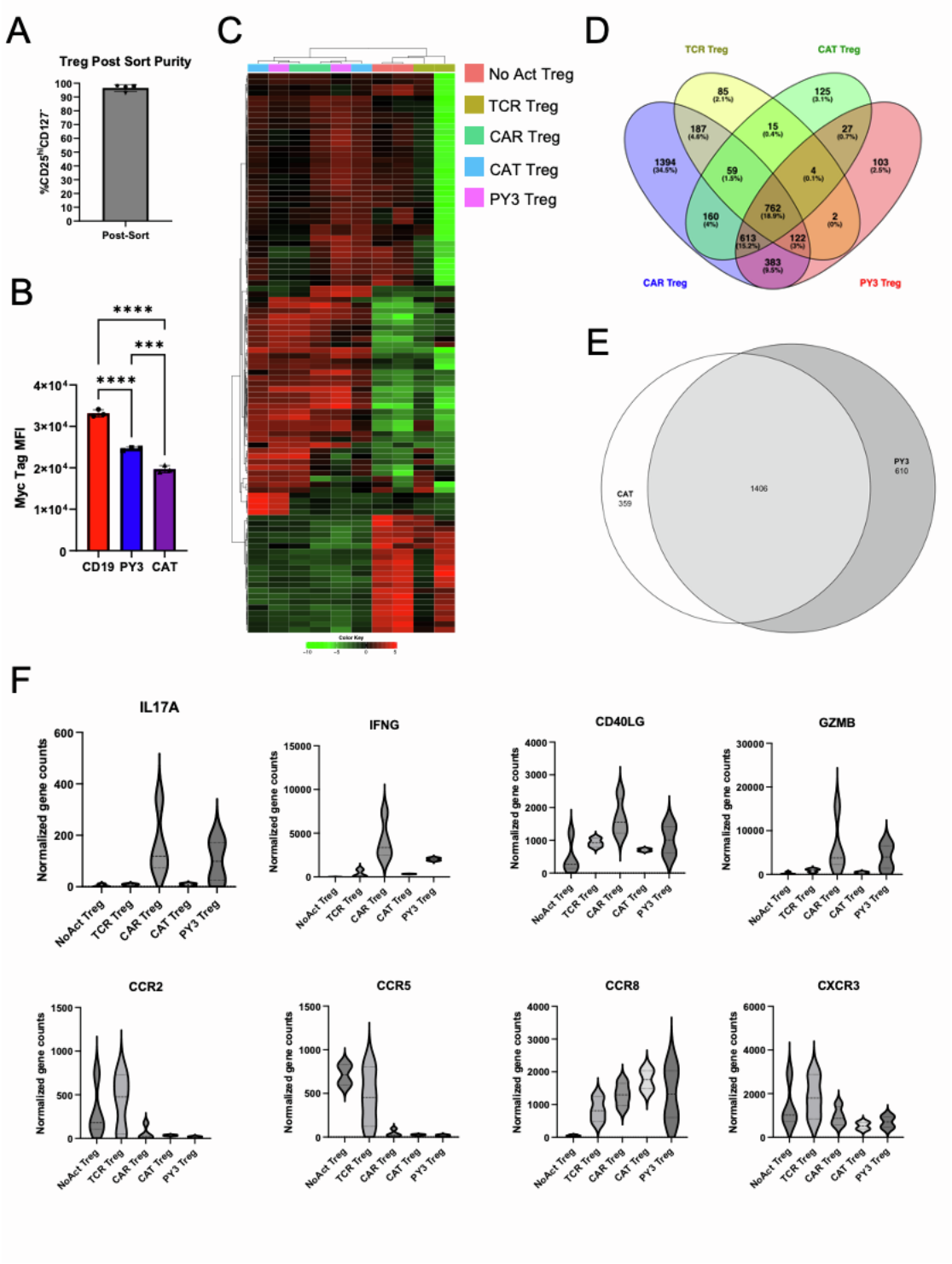
A
Treg Post Sort Purity
%CD25hiCD127-
Post-Sort
B
Myc Tag MFI
CD19 PY3 CAT
C
No Act Treg
TCR Treg
CAR Treg
CAT Treg
PY3 Treg
D
TCR Treg
CAT Treg
CAR Treg
PY3 Treg
E
CAT
359
1406
PY3
610
F
IL17A
IFNG
CD40LG
GZMB
CCR2
CCR5
CCR8
CXCR3
Normalized gene counts
NoAct Treg
TCR Treg
CAR Treg
CAT Treg
PY3 Treg

**Figure S6. CAT Tregs have lower inflammatory gene expression levels than CAR Tregs**. (A) Post-sort purity of CD25hiCD127low Tregs across multiple donors (n=4). (B) Surface expression (Myc-tag) of FMC63 CD19 CAR (CAR), CAT-13.1E10 CD19 CAR (CAT), and mutated CD28 signaling domain FMC63 CD19 CAR (PY3). Bars represent mean +/- SD of technical replicates of representative experiment, with statistical significance computed by one-way ANOVA with Tukey's multiple comparison correction. (C) Heatmap clustered by column (sample) and by row (gene) with top 100 most differentially expressed genes between No Act Tregs, TCR Tregs, CAR Tregs, CAT Tregs, and PY3 Tregs. (D) Venn diagram with genes upregulated in TCR Tregs, CAR Tregs, CAT Tregs, and PY3 Tregs in relation to their respective No Act cell types. Number of genes and respective percentage of the total number of genes are indicated in each intersection. (E) Venn diagram with genes upregulated in CAT Tregs and in PY3 Tregs. (F) Inflammatory, cytotoxic, and chemokine receptor gene expression levels in No Act Tregs, TCR Tregs, CAR Tregs, CAT Tregs, and PY3 Tregs. Violins represent mean ± standard deviation (SD) of RNA-seq gene counts from different blood donors.

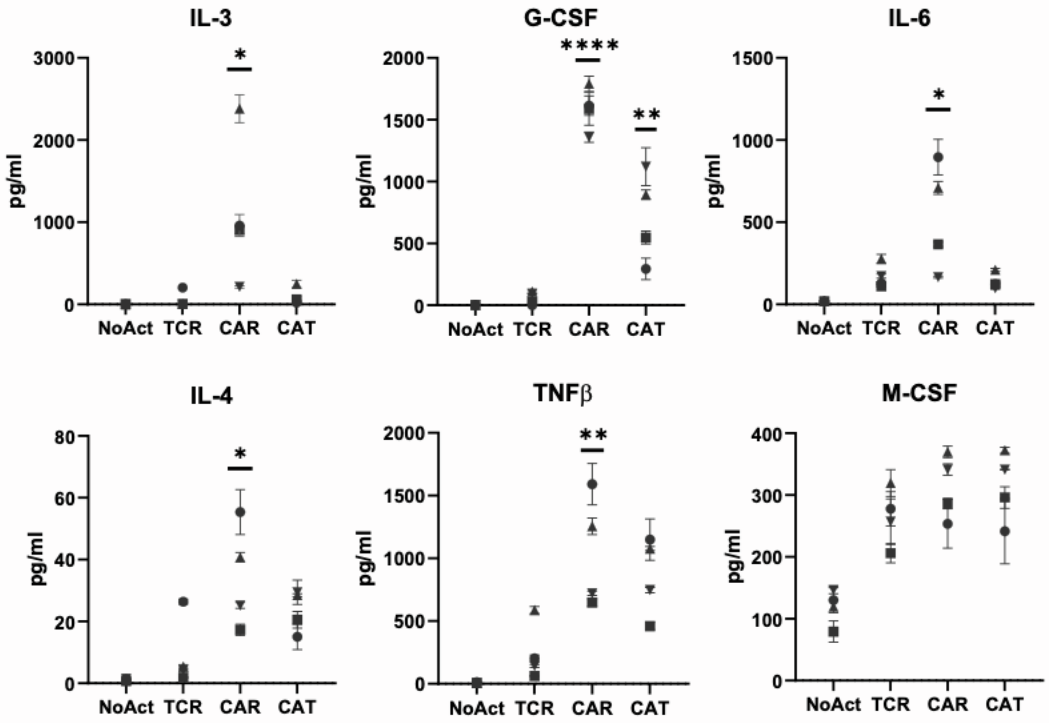
IL-3
G-CSF
IL-6
IL-4
TNFβ
M-CSF
pg/ml
NoAct
TCR
CAR
CAT
*
****
**

**Figure S7. Lowering CAR affinity leads to lower cytokine secretion.** Cytokine secretion levels by No Act Tregs, TCR Tregs, CAR Tregs, and CAT Tregs 48 hours post activation. Values are the mean ± standard deviation (SD) of technical triplicates per blood donor (n=4), with statistical significance assessed by one-way ANOVA with Tukey's multiple comparison correction. ****, $p < 0.0001$; ***, $p < 0.001$; **, $p < 0.01$; *, $p < 0.05$; ns, not significant.

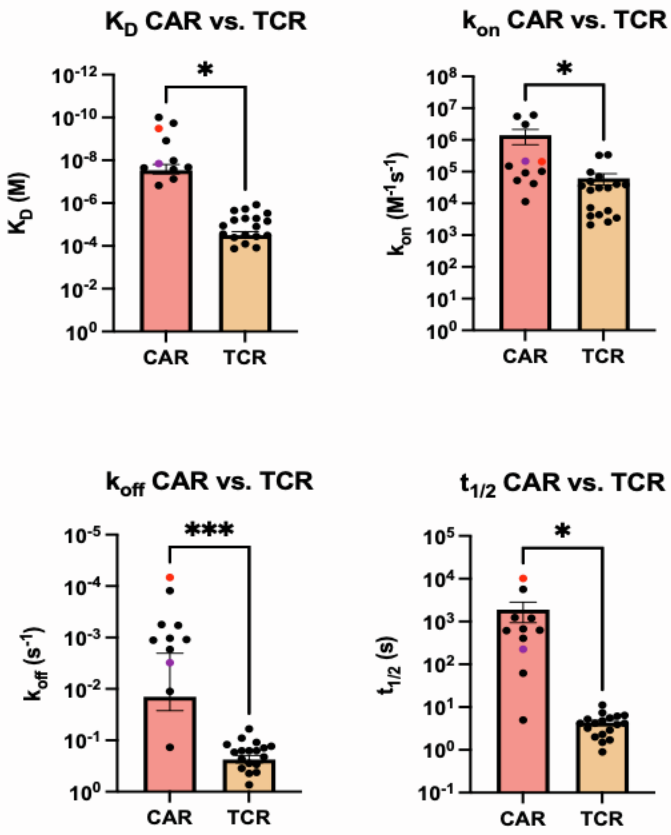
$K_D$ CAR vs. TCR
$k_{on}$ CAR vs. TCR
$k_{off}$ CAR vs. TCR
$t_{1/2}$ CAR vs. TCR
$K_D$ (M)
$k_{on}$ ($M^{-1}s^{-1}$)
$k_{off}$ ($s^{-1}$)
$t_{1/2}$ (s)
CAR
TCR
*
***

**Figure S8. Chimeric antigen receptors have a higher affinity to their cognate antigens than T cell receptors**. Dissociation constant ($K_d$), association rate constant ($k_{on}$), dissociation rate constant ($k_{off}$), and residence time ($t_{1/2}$) values for commonly used chimeric antigen receptors (CARs) to their respective targets, and well-studied T cell receptors (TCRs) to their respective cognate peptide-MHC complexes from the literature. Red dots represent FMC63 CD19 CAR (CAR) and purple dots represent CAT-13.1E10 CD19 CAR (CAT). Bars represent mean ± standard error of the mean (SEM), with statistical significance assessed by unpaired Student's t test. ****, $p < 0.0001$; ***, $p < 0.001$; **, $p < 0.01$; *, $p < 0.05$; ns, not significant.

**SUPPLEMENTAL TABLES**

**Table S1. Differentially expressed genes in CAR Tregs compared with NoAct Tregs.**

**Table S2. Differentially expressed genes in TCR Tregs compared with NoAct Tregs.**

**Table S3. Differentially expressed genes in CAR Teff compared with NoAct Teff.**

**Table S4. Differentially expressed genes in TCR Teff compared with NoAct Teff.**

**Table S5. Differentially expressed genes in CAR Tregs compared with TCR Tregs.**

**Table S6. Genes upregulated in CAR Tregs, CAR Teff, and TCR Teff, but not in TCR Tregs.**

**Table S7. Genes upregulated only in TCR Tregs and not in CAR Tregs, CAR Teff or TCR Teff.**

**Table S8. Genes upregulated in PY3 Tregs and not in CAT Tregs.**

**Table S9. Flow cytometry antibodies and dyes used in this study.**

| Antigen | Clone | Fluorophore | Dilution | Vendor | Catalog # |
|---|---|---|---|---|---|
| CD4 | SK3 | FITC | 1:100 | BioLegend | 980802 |
| CD4 | SK3 | Pacific Blue | 1:100 | BioLegend | 344619 |
| CD4 | SK3 | Alexa Fluor 700 | 1:100 | BioLegend | 344621 |
| CD4 | SK3 | PE-Cy7 | 1:100 | BioLegend | 344611 |
| CD8 | SK1 | PE | 1:100 | BioLegend | 344706 |
| CD8 | SK1 | PerCP | 1:100 | BioLegend | 344707 |
| CD25 | BC96 | APC | 1:100 | BioLegend | 302610 |
| CD45RA | HI100 | PE | 1:100 | BioLegend | 304107 |
| CD45RO | UCHL1 | BV421 | 1:100 | BioLegend | 304223 |
| CD71 | CY1G4 | PE | 1:100 | BioLegend | 334105 |
| CD80 | 2D10 | APC | 1:100 | BioLegend | 305220 |
| CD83 | HB15e | Brilliant Violet 421 | 1:100 | BioLegend | 305324 |
| CD86 | IT2.2 | PE | 1:100 | BioLegend | 305406 |
| CD127 | A019D5 | PE | 1:100 | BioLegend | 351304 |
| CD127 | A019D5 | FITC | 1:100 | BioLegend | 351311 |

| | | | | | |
|---|---|---|---|---|---|
| CD154 | 24-31 | APC | 1:100 | Biolegend | 310809 |
| CellTrace Violet | N/A | CellTrace Violet | 1:1000 | ThermoFisher | C34571 |
| CellTrace Far Red | N/A | CellTrace Far Red | 1:350 | ThermoFisher | C34572 |
| FOXP3 | PCH101 | eFluor 450 | 1:50 | eBioscience | 48-4776-42 |
| FOXP3 | PCH101 | PE/Cy5.5 | 1:50 | ThermoFisher | 35-4776-42 |
| Ghost | N/A | Red 780 | 1:500 | Tonbo Biosciences | 13-0865-T500 |
| HELIOS | 22F6 | PE | 1:50 | BioLegend | 137216 |
| IFNG | 4S.B3 | BV510 | 1:50 | Biolegend | 502543 |
| IL2 | MQ1-17H12 | Alexa Fluor 647 | 1:50 | Biolegend | 500315 |
| Live-or-Dye | N/A | 594/614 | 1:500 | Biotium | 32006 |
| MYC-tag | 9B11 | Alexa Fluor 647 | 1:100 | Cell Signaling Technologies | 2233S |
| TIGIT | A15153G | Brilliant Violet 785 | 1:100 | Biolegend | 372735 |

**Table S10. Primers used in this study.**

| Gene | Direction | Oligo sequence (5' to 3') |
|---|---|---|
| Human IFNG | FW | TCCCATGGGTTGTGTGTTTA |
| Human IFNG | REV | AAGCACCAGGCATGAAATCT |
| Human GZMB | FW | GGTGGCTTCCTGATACGAGACG |
| Human GZMB | REV | GGTCGGCTCCTGTTCTTTGAT |
| Human CD40LG | FW | GCGGCACATGTCATAAGTGAGG |
| Human CD40LG | REV | GTCCTTGTCTTTTAACGGTCAGC |
| Human TIGIT | FW | TGGTGGTCATCTGCACAGCAGT |
| Human TIGIT | REV | TTTCTCCTGAGGTCACCTTCCAC |
| Human TBX21 | FW | ATTGCCGTGACTGCCTACCAGA |
| Human TBX21 | REV | GGAATTGACAGTTGGGTCCAGG |
| Human GATA3 | FW | ACCACAACCACACTCTGGAGGA |
| Human GATA3 | REV | TCGGTTTCTGGTCTGGATGCCT |
| Human RORC | FW | GAGGAAGTGACTGGCTACCAGA |
| Human RORC | REV | GCACAATCTGGTCATTCTGGCAG |
| Human STAT1 | FW | GGCAAAGAGTGATCAGAAACAA |
| Human STAT1 | REV | GTTCAGTGACATTCAGCAACTC |
| Human RPL13a | FW | CATAGGAAGCTGGGAGCAAG |
| Human RPL13a | REV | GCCCTCCAATCAGTCTTCTG |

**Table S11. Sequences of constructs used in this study.**